MOLECULAR AND CELLULAR BIOLOGY, May 2009, p. 2372–2389 Vol. 29, No. 9
0270-7306/09/$08.00+0 doi:10.1128/MCB.01505-08

Similar and Distinct Properties of MUPP1 and Patj, Two Homologous PDZ Domain-Containing Tight-Junction Proteins▽†

Makoto Adachi,[1]* Yoko Hamazaki,[1,2] Yuka Kobayashi,[1,3] Masahiko Itoh,[1,4] Sachiko Tsukita,[1,5] Mikio Furuse,[1,6] and Shoichiro Tsukita[1]

Department of Cell Biology, Faculty of Medicine, Kyoto University, Sakyo-ku, Kyoto 606-8501, Japan[1]; Department of Immunology and Cell Biology, Graduate School of Medicine, Kyoto University, Sakyo-ku, Kyoto 606-8501, Japan[2]; Research Unit for Immune Surveillance, RIKEN Research Center for Allergy and Immunology, Yokohama, Kanagawa 230-0045, Japan[3]; Division of Molecular and Cell Biology, Institute for Medical Science, Dokkyo University School of Medicine, Mibu-machi, Tochigi 321-0293, Japan[4]; Laboratory of Biological Science, Graduate School of Frontier Biosciences/Department of Pathology, Graduate School of Medicine, Osaka University, Suita, Osaka 565-0871, Japan[5]; and Division of Cellular and Molecular Medicine, Kobe University Graduate School of Medicine, Chuo-ku, Kobe 650-0017, Japan[6]

Received 26 September 2008/Returned for modification 27 October 2008/Accepted 17 February 2009

MUPP1 and Patj are both composed of an L27 domain and multiple PDZ domains (13 and 10 domains, respectively) and are localized to tight junctions (TJs) in epithelial cells. Although Patj is known to be responsible for the organization of TJs and epithelial polarity, characterization of MUPP1 is lacking. In this study, we found that MUPP1 and Patj share several binding partners, including JAM1, ZO-3, Pals1, Par6, and nectins (cell-cell adhesion molecules at adherens junctions). MUPP1 and Patj exhibited similar subcellular distributions, and the mechanisms with which they localize to TJs also appear to overlap. Despite these similarities, functional studies have revealed that Patj is indispensable for the establishment of TJs and epithelial polarization, whereas MUPP1 is not. Thus, although MUPP1 and Patj share several molecular properties, their functions are entirely different. We present evidence that the signaling mediated by Pals1, which has a higher affinity for Patj than for MUPP1 and is involved in the activation of the Par6-aPKC complex, is of principal importance for the function of Patj in epithelial cells.

The integrity of epithelial cells is mediated by adhesive interaction at the apical junctional complex which involves tight junctions (TJs), adherens junctions (AJs), desmosomes, and gap junctions (19). TJs are located most apically and have important roles in the development and maintenance of epithelial integrity. Thus, they seal epithelial cells to create a primary barrier to the diffusion of solutes across the cellular sheet (barrier function) and serve as a boundary between the apical and basolateral membrane domains to establish polarization (fence function) (3, 26, 60, 74). Upon examination by freeze fracture replica electron microscopy, TJs appear as a set of continuous strands or fibrils of anastomosing intramembranous particles within the plasma membranes (TJ strands) (65). Their molecular architecture has been unraveled rapidly in recent years and it is now widely accepted that they are mainly composed of claudins, which bear four transmembrane domains and comprise a multigene family consisting of 24 members in both humans and mice (20, 74). In addition, three other classes of integral membrane proteins are concentrated at TJ strands, i.e., occludin (21), JAM family members (13, 44), and tricellulin, which is mostly concentrated at the tricellular contacts of TJs (31).

There are plenty of peripheral membrane proteins at TJs, and in general they possess several protein-protein interaction domains and act as molecular scaffolds that cross-link a number of TJ-associated proteins (47, 74). Among them, ZO-1, ZO-2, and ZO-3 are MAGUK family proteins that have three PDZ (*P*SD95/*D*lg/*Z*O-1) domains, one Src homology (SH3) domain, and one guanylate kinase-like (GUK) domain. Through these domains, they directly bind to transmembrane proteins, including occludin, claudins, and JAM, and other peripheral membrane proteins such as ZONAB and cingulin, as well as to the actin cytoskeleton (24, 54, 74).

Several proteins regulating epithelial cell polarity have been identified at TJs. They include the Par3-Par6-atypical protein kinase C (aPKC) complex, which was initially found in a study of anterior-posterior polarity in the early *Caenorhabditis elegans* embryo, and the Crb-Pals1-Patj complex, which was initially identified in *Drosophila* flies (7, 14, 18, 23, 28, 36, 45, 69, 78). Genetic studies of *Drosophila* flies have suggested the occurrence of complex functional interactions between these two complexes: the Par3-Par6-aPKC complex provides for the apical localization of the Crb-Pals1-Patj complex, and the Crb-Pals1-Patj complex prevents the Par3-Par6-aPKC complex from diffusing into lateral membranes (11, 73). Such functional interactions have not been demonstrated in studies of mammals, but physical interactions between Pals1 and Par6 and between Crb and Par6 (in mammals) and between Crb and aPKC, Par6 and Patj, and aPKC and Patj (in *Drosophila* flies) have been previously reported (22, 30, 41, 49, 64) and might underlie the functional interactions between these two complexes.

* Corresponding author. Mailing address: Department of Cell Biology, Faculty of Medicine, Kyoto University, Sakyo-ku, Kyoto 606-8501, Japan. Phone: 81-75-753-4375. Fax: 81-75-753-4660. E-mail: ada@mfour.med.kyoto-u.ac.jp.

† Supplemental material for this article may be found at http://mcb.asm.org/.

▽ Published ahead of print on 2 March 2009.

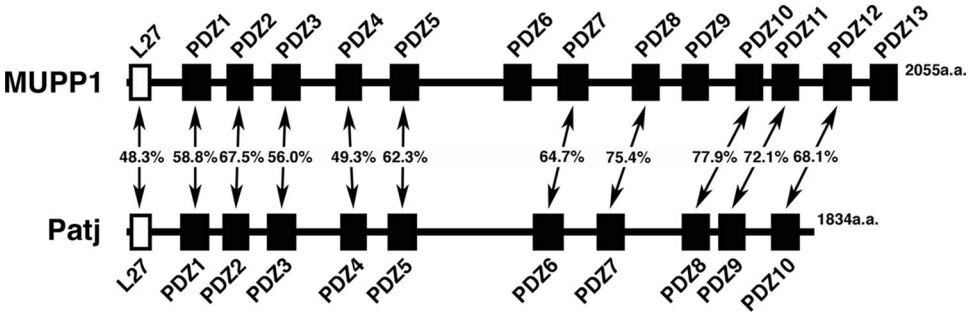

FIG. 1. Schematic representation of MUPP1 and Patj. MUPP1 has an L27 domain and 13 PDZ domains, whereas Patj has an L27 domain and 10 PDZ domains. Amino acid sequence identity between the respective L27 and PDZ domains is also shown. Note that Patj does not harbor the domains that correspond to PDZ6, -9, and -13 of MUPP1. Identity values were calculated using Genetyx Mac software.

We have previously shown that MUPP1, which possesses an L27 domain and 13 PDZ domains, is a novel component of TJs and directly binds to claudin-1 and JAM1 (Fig. 1) (27). MUPP1 was originally identified as a binding partner for serotonin 5-hydroxytryptamine type 2 receptor (63, 75) and is also known to bind to c-Kit, transmembrane proteoglican NG2, adenovirus E4-ORF1, and high-risk papillomavirus type 18 E6 oncoproteins (9, 39, 43). Importantly, Patj is a structural paralogue of MUPP1 with an L27 domain and 10 PDZ domains (Fig. 1) (40, 58). Patj is important for the polarization of photoreceptor cells in *Drosophila* flies (10, 50, 53, 56) and is critical for the establishment of epithelial polarity in mammals (30, 46, 58, 61). However, the functional characterization of MUPP1 has largely been lacking.

In this study, we found that MUPP1 and Patj share several binding partners, including JAM1, ZO-3, and Pals1, which have been reported to directly bind to either of the two proteins. In addition, we identified novel binding partners for MUPP1 and Patj, i.e., nectins, cell-cell adhesion molecules of AJs, and Par6, a principal regulator of polarity. These binding partners might well be important for the functions or regulation of MUPP1 and Patj, and the sharing of many binding partners strongly suggests that MUPP1 and Patj have similar molecular characteristics. Surprisingly, functional analyses have clearly revealed that these two proteins have entirely distinct functions; Patj evidently plays an essential role in the formation of TJs and epithelial polarity, whereas MUPP1 does not. In fact, MUPP1 and Patj had significant molecular differences that might well underlie their functional differences. In particular, MUPP1 had a higher affinity for nectins than Patj, whereas Patj preferentially bound to Pals1 and Par6. It was then found that a truncated mutation of Patj whose binding domain for Pals1 was deleted was unable to rescue the defects in TJs in Patj-knockdown cells. Taking these findings together with other corroborative data, we speculate that Pals1-mediated signaling, which is involved in the regulation of the Par6-aPKC complex, is of principal importance for the predominant function of Patj in epithelial cells.

MATERIALS AND METHODS

Antibodies and cells. Rabbit anti-MUPP1 polyclonal antibody (PAb) (B4) (27), mouse anti-ZO-1 monoclonal antibody (MAb) (clone no. T8-754) (34), and rabbit anti-JAM1 PAb (33) were generated and characterized previously. Rabbit anti-Pals1 antiserum was raised against amino acids (aa) 1 to 122 of mouse Pals1. Rabbit anti-claudin-1 PAb, rabbit anti-claudin-3 PAb, mouse anti-claudin-4 MAb, and mouse anti-myc MAb (clone no. 9E10; Zymed Laboratories, Inc.), mouse anti-MUPP1 MAb (clone 43; BD Transduction Laboratories, Inc.), rabbit anti-PKCζ PAb (C20) and rabbit anti-myc PAb (A14) (Santa Cruz Laboratories, Inc.), rabbit anti-Par3 PAb (Upstate Biotechnologies, Inc.), and mouse anti-HA MAb (16B12) (Covance) were obtained commercially. Rat anti-nectin-2 MAb (5) was provided by Y. Takai (Kobe University, Kobe, Japan) and H. Nakanishi (Kumamoto University, Kumamoto, Japan), rabbit anti-Patj PAb (40) was provided by A. Le Bivic (University of Marseille, Marseille, France), and rabbit anti-Par6B PAb (BC32AP) was provided by S. Ohno (Yokohama City University, Yokohama, Japan). Mouse mammary gland EpH4 cells were provided by E. Reichmann (University Children's Hospital Zurich, Zurich, Switzerland). EpH4 cells, HEK293 cells, L cells, L cells stably expressing full-length nectin-2α (nectin-2α-L cells [referred to as NL cells in this paper]) (71), and L cells stably expressing nectin-2α lacking the PDZ-binding motif AVYV (nectin-2α-ΔC-L cells [referred to as NLΔAVYV cells in this paper]) (48) were cultured in Dulbecco's modified Eagle's medium supplemented with 10% fetal calf serum. Mouse F9 teratocarcinoma cells were cultured under the same conditions, and epithelial differentiation was induced in monolayer cultures by adding retinoic acid to the culture medium at a final concentration of 1 μM (29).

DNA constructs. To obtain a full-length cDNA fragment of mouse Patj, the open reading frame (ORF) of human Patj was used to perform a search of the public mouse EST database. Examination of several expressed sequence tag (EST) clones has revealed that the ORF of mouse Patj is 5,505 bp in length and that the amino acid sequence of mouse Patj is 79% identical to that of human Patj. To obtain the full-length Patj cDNA, an XhoI-SalI fragment containing bp 1 to 1726 of the ORF (obtained by reverse transcription-PCR [RT-PCR] of mouse brain cDNA), a SalI-EcoRV fragment of bp 1726 to 5200 of the ORF (derived from a RIKEN FANTOM cDNA clone [clone identification no. 5031439B21] carrying bp 1689 to 5505 for mouse Patj), and an EcoRV-XhoI fragment of bp 5200 to 5502 of the ORF (lacking a stop TAA codon; obtained by PCR of the FANTOM clone) were sequentially ligated. It was cloned into the mammalian expression vector pCAGGS, whose multiple cloning site (MCS) was tagged on the 3′ side with 7xmyc (pCAGGS-3′-7xmyc), yielding pCAGGS-Patj-myc. pCAGGS-MUPP1-myc, a mammalian expression vector for mouse MUPP1 tagged with 7xmyc, was described previously (27). The following PDZ domains of Patj were amplified by PCR: PDZ1 (aa 119 to 231), PDZ2 (aa 233 to 338), PDZ3 (aa 350 to 463), PDZ4 (aa 540 to 651), PDZ5 (aa 673 to 776), PDZ6 (aa 1059 to 1176), PDZ7 (aa 1230 to 1338), PDZ8 (aa 1457 to 1565), PDZ9 (aa 1553 to 1660), and PDZ10 (aa 1694 to 1805). EcoRI-SalI cDNA fragments for each PDZ domain were subcloned into pBTM116, a bait vector for two-hybrid analysis, and pMAL-c2 (New England Biolabs Inc.), an expression vector for maltose-binding protein (MBP)-fused proteins in *Escherichia coli*. EcoRI-SalI fragments for the following domains of Patj were also inserted into the MCS of pMAL-c2: PDZ1 to -5 (aa 119 to 776), PDZ6 to -10 (aa 1059 to 1805), PDZ1 to -3 (aa 119 to 463), PDZ4 and -5 (aa 540 to 776), PDZ6 and -7 (aa 1059 to 1338), and PDZ8 to -10 (aa 1457 to 1805). PDZ domain constructs of MUPP1 were previously described (27). The expression vector for MUPP1ΔPDZ2,3,4,5-myc was obtained by ligating a NotI-XhoI fragment (for aa 1 to 265) and an XhoI-SalI fragment (for aa 781 to 2055) into the MCS of pCAGGS-3′-7xmyc, and the expression vector for MUPP1ΔPDZ2,5-myc was obtained by inserting an XhoI-XhoI fragment (for aa 339 to 700) into the XhoI site of MUPP1ΔPDZ2,3,4,5-myc. The ORF of PatjΔL27 was obtained by ligating an EcoRI fragment (for aa 119 to 317) and an EcoRI-XhoI fragment (for aa 318 to 1834, containing mutations for RNA interference [RNAi] resistance). The ORF of PatjΔ2,5 was yielded by ligating a

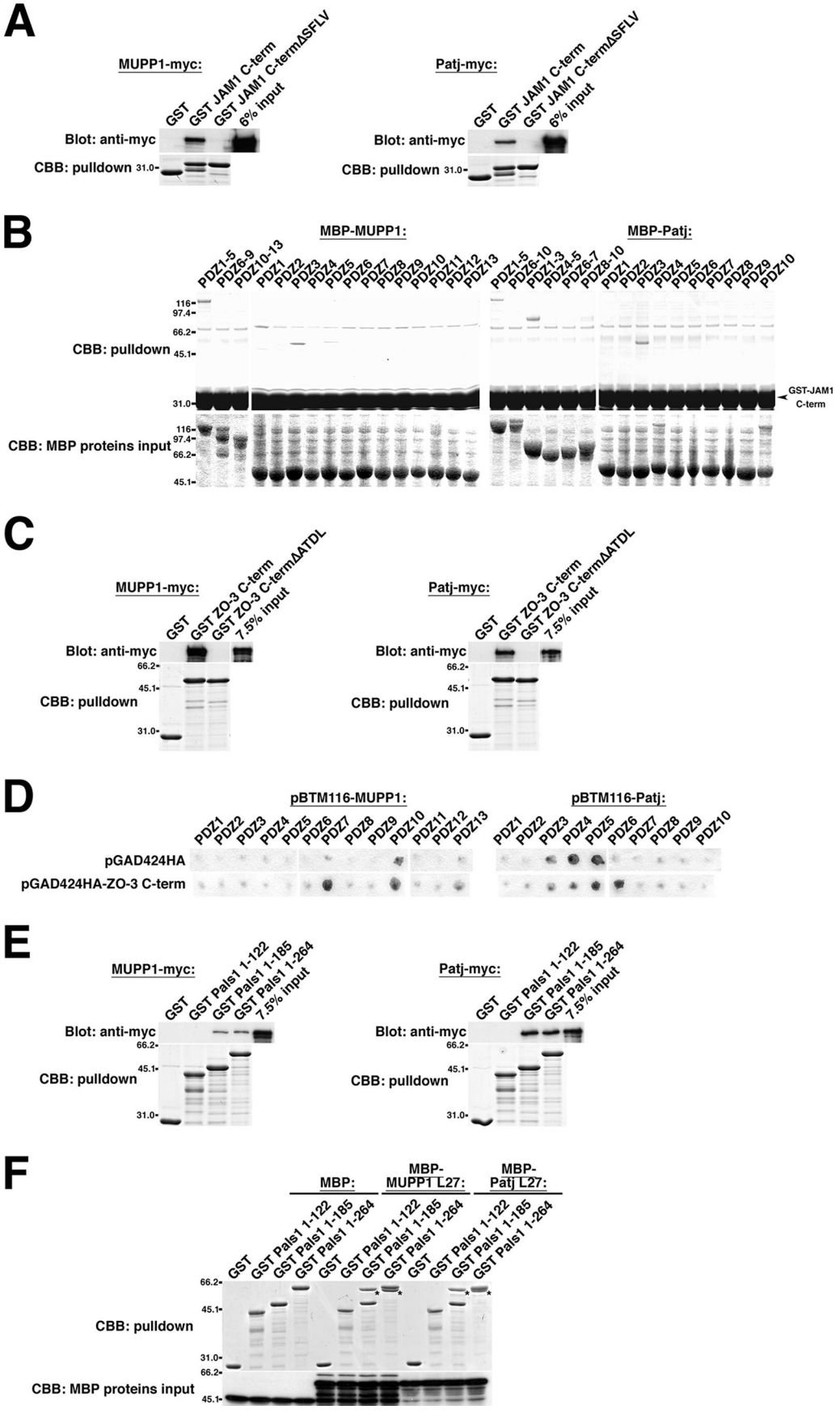
A
MUPP1-myc:
GST
GST JAM1 C-term
GST JAM1 C-termΔSFLV
6% input
Blot: anti-myc
CBB: pulldown
31.0
Patj-myc:
GST
GST JAM1 C-term
GST JAM1 C-termΔSFLV
6% input
Blot: anti-myc
CBB: pulldown
31.0
B
MBP-MUPP1:
PDZ1-5
PDZ6-9
PDZ10-13
PDZ1
PDZ2
PDZ3
PDZ4
PDZ5
PDZ6
PDZ7
PDZ8
PDZ9
PDZ10
PDZ11
PDZ12
PDZ13
MBP-Patj:
PDZ1-5
PDZ6-10
PDZ1-3
PDZ4-5
PDZ6-7
PDZ8-10
PDZ1
PDZ2
PDZ3
PDZ4
PDZ5
PDZ6
PDZ7
PDZ8
PDZ9
PDZ10
116
97.4
66.2
45.1
31.0
CBB: pulldown
GST-JAM1 C-term
CBB: MBP proteins input
C
MUPP1-myc:
GST
GST ZO-3 C-term
GST ZO-3 C-termΔATDL
7.5% input
Blot: anti-myc
66.2
45.1
31.0
CBB: pulldown
Patj-myc:
GST
GST ZO-3 C-term
GST ZO-3 C-termΔATDL
7.5% input
Blot: anti-myc
66.2
45.1
31.0
CBB: pulldown
D
pBTM116-MUPP1:
PDZ1
PDZ2
PDZ3
PDZ4
PDZ5
PDZ6
PDZ7
PDZ8
PDZ9
PDZ10
PDZ11
PDZ12
PDZ13
pBTM116-Patj:
PDZ1
PDZ2
PDZ3
PDZ4
PDZ5
PDZ6
PDZ7
PDZ8
PDZ9
PDZ10
pGAD424HA
pGAD424HA-ZO-3 C-term
E
MUPP1-myc:
GST
GST Pals1 1-122
GST Pals1 1-185
GST Pals1 1-264
7.5% input
Blot: anti-myc
66.2
45.1
31.0
CBB: pulldown
Patj-myc:
GST
GST Pals1 1-122
GST Pals1 1-185
GST Pals1 1-264
7.5% input
Blot: anti-myc
66.2
45.1
31.0
CBB: pulldown
F
MBP:
MBP-MUPP1 L27:
MBP-Patj L27:
GST
GST Pals1 1-122
GST Pals1 1-185
GST Pals1 1-264
66.2
45.1
31.0
CBB: pulldown
66.2
45.1
CBB: MBP proteins input

NotI-XhoI fragment (for aa 1 to 255), an XhoI-XhoI fragment (for aa 329 to 695), and an XhoI-SalI fragment (for aa 776 to 1834, containing mutations for RNAi resistance). The ORF of PatjΔPDZ4 was obtained by ligating a NotI-XhoI fragment (for aa 1 to 570) and an XhoI-XhoI fragment (for aa 642 to 1834). These ORFs were inserted into the MCS of pCAGGS-3′-7xmyc. EcoRI-BamHI fragments of the cytoplasmic domain of human nectin-1α (for aa 379 to 518) and mouse nectin-2α (for aa 387 to 467) were amplified by PCR and subcloned into pGAD424HA (Clontech Laboratories, Inc.), yielding prey vectors for two-hybrid analysis (66). *E. coli* expression vectors for the glutathione *S*-transferase (GST)-fused (pGEX vectors) cytoplasmic domains of human nectin-1α and mouse nectin-2α (provided by Y. Takai and H. Nakanishi), cytoplasmic domain of human JAM1 (aa 261 to 299), and C terminus of mouse ZO-3 (aa 758 to 905) were described previously (32, 33, 59, 71). An XhoI-BamHI fragment for the cytoplasmic domain of JAM1 and an EcoRI-SalI fragment for the C terminus of ZO-3 lacking four amino acids of the PDZ-binding motif were ligated into pGEX vectors to yield pGEX JAM1 C-termΔSFLV and pGEX ZO-3 C-termΔATDL, respectively. EcoRI-SalI fragments of the N-terminal L27 domains of MUPP1 and Patj (aa 1 to 142 and aa 1 to 138, respectively) were amplified by PCR and ligated into pMAL-c2 and pCAGGS-5′-7xmyc, yielding pMAL-MUPP1-L27, pMAL-Patj-L27, pCAGGS-myc-MUPP1-L27, and pCAGGS-myc-Patj-L27. ORFs of mouse Par3 (a SalI-EcoRI fragment), mouse Par6A (an XhoI-XhoI fragment), human Par6B (an EcoRI-EcoRI fragment), and mouse PKCζ (an EcoRI-EcoRI fragment) were amplified by PCR and subcloned into either pCAGGS-5′-hemagglutinin (pCAGGS-5′-HA) or pGEX-4T1, yielding pCAGGS-HA-Par3, pCAGGS-HA-Par6A, pCAGGS-HA-Par6B, pCAGGS-HA-PKCζ, and pGEX-Par6A. Several fragments encoding portions of Par6A, aa 1 to 132, aa 1 to 155, and aa 1 to 382 (XhoI-XhoI fragments) and aa 99 to 382, aa 144 to 382, and aa 254 to 382 (XhoI-SalI fragments), were amplified by PCR and ligated into pGEX-4T1, yielding several deletion constructs for Par6A. Similarly, fragments encoding portions of mouse Pals1, aa 1 to 122, aa 1 to 185, and aa 1 to 264 (EcoRI-XhoI fragments), were amplified and ligated into pGEX-4T1. An EcoRI-EcoRI fragment of the N-terminal regulatory domain (RD) of mouse PKCζ (for aa 1 to 256) was ligated into pColdI (TaKaRa) to yield an *E. coli* expression vector for His-PKCζ RD, pColdI-PKCζ RD. Mammalian expression vectors for constitutively active forms of Cdc42 and Rac1, pEF-myc-Cdc42G12V and pEF-myc-Rac1G12V, respectively, were provided by Y. Takai.

In vitro pulldown assay. The recombinant GST-, His-, and MBP-fused proteins were expressed in *E. coli* BL21(pLysS) except for GST-nectin-1α C-term and GST-JAM1 C-term, which were expressed in Rosetta blue (Novagen) and *E. coli* BL21 harboring pTf16, an expression vector for the trigger factor (TaKaRa), respectively. GST-fused proteins were bound to glutathione-Sepharose 4B beads (Amersham Biosciences, Inc.) and incubated with lysates of *E. coli* expressing MBP-fused proteins. They were washed with phosphate-buffered saline (PBS) containing 1% Triton X-100, and bound proteins were eluted with sodium dodecyl sulfate-polyacrylamide gel electrophoresis sample buffer. Alternatively, HEK293 cells were transfected with MUPP1-myc or Patj-myc and lysed with lysis buffer (20 mM Tris-HCl [pH 7.5], 150 mM NaCl, 1% Triton X-100, 10 mM NaF, 12.5 mM β-glycerophosphate, 1 mM Na_3VO_4, 1 mM phenylmethylsulfonyl fluoride, 0.25% aprotinin, 1 mM dithiothreitol). The lysates were incubated with beads, washed with lysis buffer, and then eluted as described above.

Yeast two-hybrid analysis. The methodology of yeast two-hybrid screening was described previously (27, 67). By the use of LexA-binding domain-fused constructs (pBTM116) of PDZ1, PDZ2, PDZ3, PDZ5, PDZ8, and PDZ12 of MUPP1 as bait, $\sim 2 \times 10^7$ clones from a mouse embryonic cDNA library (cloned in pVP16 and containing the VP16 transactivating domain) were screened. This library was provided by J. Behrens (Max-Delbruck Center for Molecular Biology, Berlin, Germany). Screening under selective conditions with pBTM116-PDZ2 used as bait yielded two positive clones, which carried the cytoplasmic domain of mouse nectin-1α (prey no. 99 [aa 381 to 515] and prey no. 456 [aa 389 to 515]). Their interaction was evaluated by measuring β-galactosidase activity on filters. To examine the interaction between nectins and the PDZ domains of MUPP1 and Patj, pVP16-nectin-1α (for aa 381 to 515; mouse) (prey no. 99), pGAD424HA-nectin-1α (for aa 379 to 518; human), nectin-2α (for aa 387 to 467; mouse), pBTM116-MUPP1-PDZ1 to -13, and pBTM116-Patj-PDZ1 to -10 were used. To evaluate the interaction between ZO-3 and MUPP1 and Patj, pGAD424HA-ZO-3 C-term (for aa 758 to 905; mouse) was used as the prey.

Immunoprecipitation. Lysates of HEK293 cells transfected with several expression constructs for HA- or myc-tagged proteins were mixed with protein G-Sepharose preabsorbed with anti-HA MAb. For immunoprecipitation of endogenous proteins, EpH4 cells were lysed with lysis buffer, and the lysates were incubated with protein G-Sepharose preabsorbed with anti-MUPP1 MAb. The beads were extensively washed with lysis buffer, and bound proteins were eluted by adding sodium dodecyl sulfate-polyacrylamide gel electrophoresis sample buffer.

Immunofluorescence microscopy. Cells plated on glass coverslips or Transwell filters (Coster) were fixed with 1% formaldehyde for 30 min at room temperature, 10% trichloroacetic acid for 30 min at 4°C, or methanol for 10 min at −20°C. After being fixed with formaldehyde or trichloroacetic acid, cells were treated with 0.2% Triton X-100 in PBS for 5 min. Cells were washed three times with PBS and soaked in PBS containing 1% bovine serum albumin. They were then incubated with primary antibodies for 1 h at room temperature or overnight at 4°C in a moist chamber. After three washes with PBS, they were incubated for 30 min at room temperature with secondary antibodies. After another three washes with PBS, they were embedded in Mowiol (Calbiochem). Specimens were examined using an Olympus BX51 photomicroscope (Olympus) or a Zeiss LSM510 confocal laser-scanning microscope (Carl Zeiss).

Wound healing assay. The wound healing assay was performed as described previously (4). Briefly, confluent EpH4 cells cultured on glass coverslips were wounded manually with 18-gauge needles. Four linear wounds were made on each coverslip. The culture medium was replaced with fresh medium, and the wounds were allowed to heal for 4, 6, or 8 h prior to the analysis.

RNAi. The targeted sequences of mouse MUPP1 and Patj were as follows: MUPP1 KD-1 (bp 396 to 414 of MUPP1 cDNA [5′-GGGTCGCCATGTGGAAATA-3′]), MUPP1 KD-2 (bp 5010 to 5028 of MUPP1 cDNA [5′-GCGAAAGGCTACACATGAT-3′]), Patj KD-1 (bp 3869 to 3887 of Patj cDNA [5′-GAGACGAGCTGCTAGAGAT-3′]), and Patj KD-2 (3′ untranslated region of mouse Patj mRNA [5′-GTGAAGTGACCAGATCTTA-3′]). DNA oligonucleotides designed from these sequences were cloned into an H1 promoter RNAi vector (12).

Measurement of TER. Aliquots of 1×10^5 cells were plated on Transwell filters 12 mm in diameter (four filters for each cell line), and the culture medium was changed every day. Transepithelial electric resistance (TER) was measured directly in the culture medium by the use of an epithelial volt-ohm meter (model Millicell-ERS; Millipore). The TER values were calculated by subtracting the background TER of blank filters and multiplying by the surface area of the filter.

FIG. 2. Interaction with JAM1, ZO-3, and Pals1. (A and B) Interaction with JAM1. (A) In vitro pulldown assay using a GST-fused C-terminal cytoplasmic domain of JAM1 (JAM1 C-term) or the cytoplasmic domain of JAM1 lacking the PDZ-binding motif, SFLV (JAM1 C-termΔSFLV), and lysates of cells expressing MUPP1-myc or Patj-myc. Bound proteins were eluted and analyzed by immunoblotting with anti-myc PAb. MUPP1 and Patj bound to JAM1 C-term, but not to JAM1 C-termΔSFLV. (B) In vitro pulldown assay using GST-JAM1 C-term and lysates of *E. coli* expressing MBP-fused PDZ domains of MUPP1 and Patj. The PDZ3 domain of MUPP1 and the PDZ3 domain of Patj specifically interacted with JAM1. (C and D) Interaction with ZO-3. (C) In vitro pulldown assay using a GST-fused C terminus of ZO-3 (ZO-3 C-term) and the C terminus of ZO-3 lacking the PDZ-binding motif, ATDL (ZO-3 C-termΔATDL), and lysates of cells expressing MUPP1-myc or Patj-myc. MUPP1 and Patj bound to ZO-3 C-term but not to ZO-3 C-termΔATDL. (D) β-Galactosidase assay using ZO-3 C-term (cloned in pGAD424 HA) and the PDZ domains of MUPP1 and Patj (in pBTM116). The PDZ7 domain of MUPP1 and the PDZ6 domain of Patj showed specific interaction with ZO-3. (E and F) Interaction with Pals1. (E) In vitro pulldown assay using GST-fused aa 1 to 122, aa 1 to 185, and aa 1 to 264 of Pals1 and lysates of cells expressing MUPP1-myc or Patj-myc. MUPP1 and Patj bound to aa 1 to 185 (containing L27N domain) and aa 1 to 264 (L27N and L27C domains), but not to aa 1 to 122 (no particular domains), of Pals1. Signals for Pals1-bound MUPP1 were weaker than those for Patj. (F) In vitro pulldown assay using GST-Pals1 constructs and the MBP-fused L27 domain of MUPP1 and Patj. MUPP1-L27 and Patj-L27 interacted with aa 1 to 185 and aa 1 to 264, but not with aa 1 to 122, of Pals1. Asterisks indicate bound MBP-fused proteins. CBB, Coomassie brilliant blue.

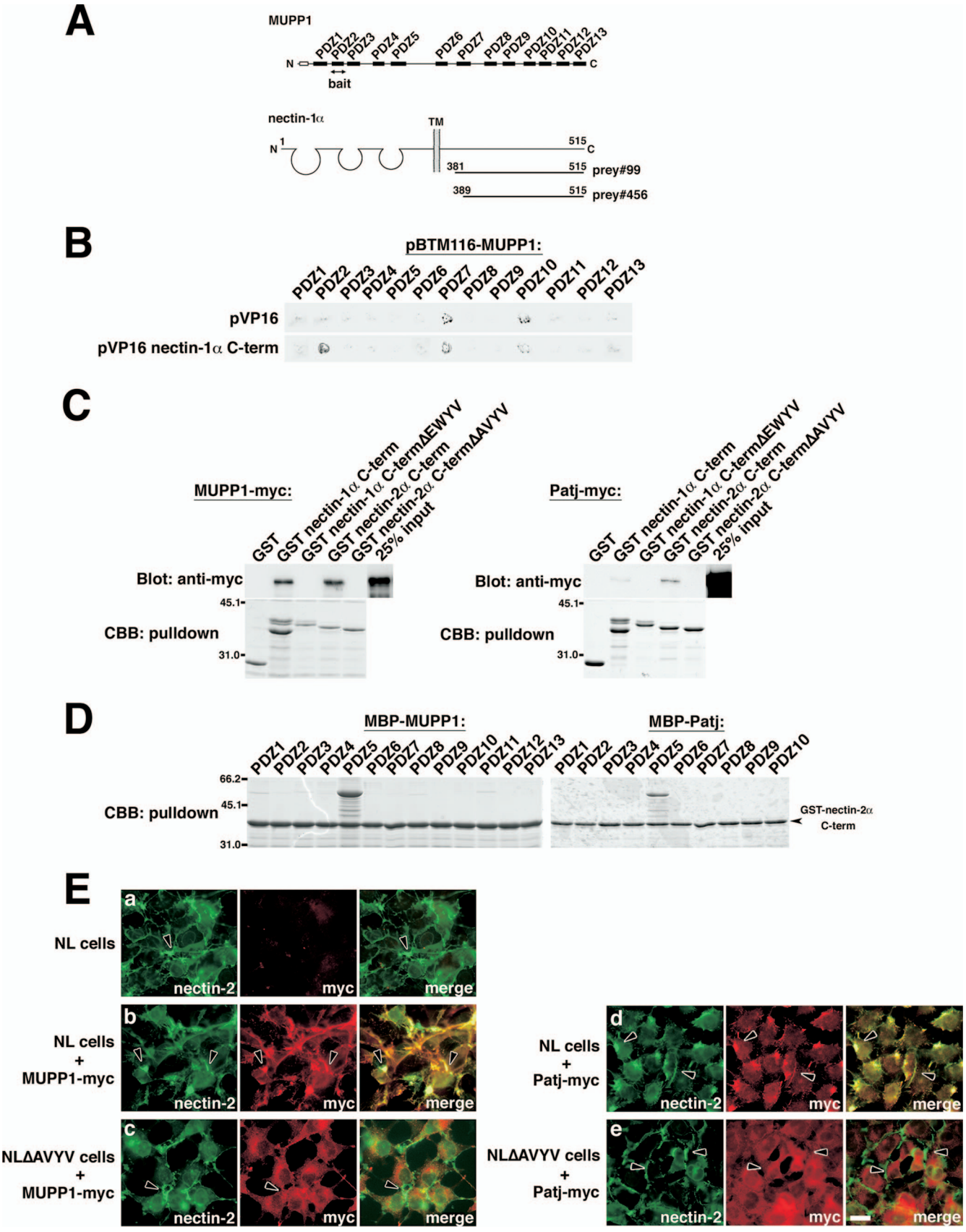
A
MUPP1
PDZ1 PDZ2 PDZ3 PDZ4 PDZ5 PDZ6 PDZ7 PDZ8 PDZ9 PDZ10 PDZ11 PDZ12 PDZ13
N
C
bait
nectin-1α
TM
N 1
515 C
381 515 prey#99
389 515 prey#456
B
pBTM116-MUPP1:
PDZ1 PDZ2 PDZ3 PDZ4 PDZ5 PDZ6 PDZ7 PDZ8 PDZ9 PDZ10 PDZ11 PDZ12 PDZ13
pVP16
pVP16 nectin-1α C-term
C
MUPP1-myc:
GST
GST nectin-1α C-term
GST nectin-1α C-termΔEWYV
GST nectin-2α C-term
GST nectin-2α C-termΔAVYV
25% input
Blot: anti-myc
45.1
CBB: pulldown
31.0
Patj-myc:
GST
GST nectin-1α C-term
GST nectin-1α C-termΔEWYV
GST nectin-2α C-term
GST nectin-2α C-termΔAVYV
25% input
Blot: anti-myc
45.1
CBB: pulldown
31.0
D
MBP-MUPP1:
PDZ1 PDZ2 PDZ3 PDZ4 PDZ5 PDZ6 PDZ7 PDZ8 PDZ9 PDZ10 PDZ11 PDZ12 PDZ13
MBP-Patj:
PDZ1 PDZ2 PDZ3 PDZ4 PDZ5 PDZ6 PDZ7 PDZ8 PDZ9 PDZ10
66.2
CBB: pulldown
45.1
31.0
GST-nectin-2α C-term
E
NL cells
a
nectin-2
myc
merge
NL cells + MUPP1-myc
b
nectin-2
myc
merge
NLΔAVYV cells + MUPP1-myc
c
nectin-2
myc
merge
NL cells + Patj-myc
d
nectin-2
myc
merge
NLΔAVYV cells + Patj-myc
e
nectin-2
myc
merge

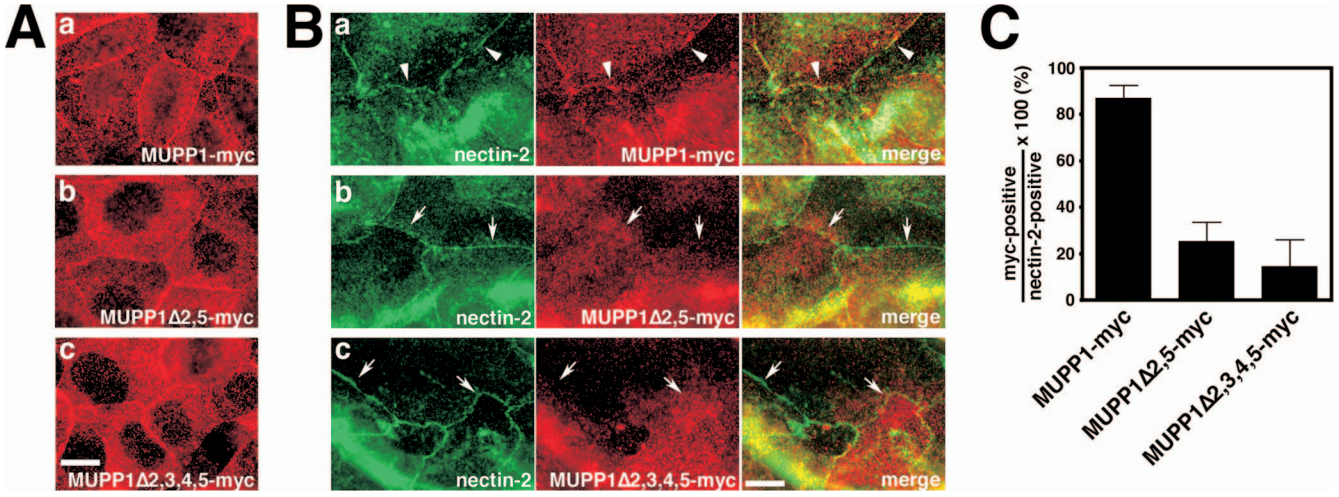

FIG. 4. Involvement of nectins in the junctional recruitment of MUPP1. (A) EpH4 cells were stably transfected with MUPP1-myc (a), MUPP1ΔPDZ2,5-myc (b), or MUPP1ΔPDZ2,3,4,5-myc (c) at comparable expression levels (data not shown) and were grown to confluence on glass coverslips. Staining with anti-myc PAb revealed that MUPP1-myc clearly localized to TJs, whereas the localization of MUPP1ΔPDZ2,5-myc and MUPP1ΔPDZ2,3,4,5-myc to TJs was slightly blurred. (B) Confluent cultures were scratched with a needle, and after culturing for 6 h, they were fixed and stained with anti-nectin-2 MAb and anti-myc PAb. MUPP1-myc accumulated at most nectin-2-positive cell-cell junctions (a [arrowheads]), whereas MUPP1ΔPDZ2,5-myc (b) and MUPP1ΔPDZ2,3,4,5-myc (c) did not (arrows). (C) Quantification of the results shown in panel B. Percentages of nectin-2-positive cell-cell junctions where the respective MUPP1 constructs were colocalized at 6 h after wounding are shown ($n = 3$).

RESULTS

Common binding partners for MUPP1 and Patj. Several binding partners for MUPP1 and Patj that have important functions in the establishment of TJs have been identified. Despite the structural similarity between MUPP1 and Patj, however, whether they can bind to the same proteins is largely unexamined. We examined the binding profile of JAM1, reported to bind to MUPP1 (27), and of ZO-3, reported to bind Patj (57). In vitro pulldown assays revealed that the cytoplasmic domain of JAM1 binds to MUPP1 and Patj with similar degrees of affinity and that this interaction was abrogated when the C-terminal four amino acids of the PDZ-binding motif of JAM1 (SFLV) were deleted (Fig. 2A). Utilization of MBP-fused PDZ domains revealed the binding domain to be PDZ3 of MUPP1 and PDZ3 of Patj (Fig. 2B; see also Discussion). ZO-3 interaction with MUPP1 as well as with Patj was dependent on its C-terminal PDZ-binding motif (ATDL), and the levels of affinity of MUPP1 and Patj were almost indistinguishable (Fig. 2C). A β-galactosidase assay utilizing the respective PDZ domains revealed that ZO-3 binds to PDZ7 of MUPP1 and PDZ6 of Patj (Fig. 2D). It should be noted that, among all the PDZ domains within these two proteins, PDZ3 and PDZ7 of MUPP1 are most similar to PDZ3 and PDZ6 of Patj, respectively (Fig. 1). Thus, MUPP1 and Patj appear to have similar properties.

It has been reported that Pals1 can bind to MUPP1, as well as to Patj, although this interaction has not been adequately characterized (58). We then found that the L27N domain of Pals1 interacted with MUPP1, although the affinity was weaker than that for Patj, and that the interaction occurred through the L27 domains of MUPP1 and Patj (Fig. 2E and F). Thus, Pals1 utilizes the same mechanism to bind to MUPP1 and to Patj.

Identification of interaction of MUPP1 and Patj with nectins. To further characterize MUPP1 and Patj, we attempted to identify novel binding partners. In a yeast two-hybrid screening using the PDZ2 domain of MUPP1 as bait, we obtained two positive clones, both of which encoded the cytoplasmic

FIG. 3. Interaction with nectin-1α and -2α. (A) Yeast two-hybrid screening for MUPP1-binding proteins with a mouse embryonic cDNA library. The PDZ2 domain of MUPP1 was used as bait, and 30 positive clones were obtained. Two of these clones encoded the C-terminal cytoplasmic domain of nectin-1α (prey no. 99 and no. 456, encoding aa 381 to 515 and aa 389 to 515, respectively). TM, transmembrane domain. (B) β-Galactosidase assay using filters and the PDZ domains of MUPP1 (in pBTM116) and the cytoplasmic domain of nectin-1α (in pVP16; prey no. 99). The PDZ2 domain of MUPP1 showed specific interaction with nectin-1α. (C) In vitro pulldown assays using a GST-fused C terminus of nectin-1α or -2α and PDZ-binding motif-deleted mutants (nectin-1α C-termΔEWYV and nectin-2α C-termΔAVYV) and lysates of cells expressing MUPP1-myc or Patj-myc. MUPP1 and Patj bound to nectin-1α and -2α but not to their PDZ-binding motif-deleted mutants. The affinity of Patj for nectins was lower than that of MUPP1. CBB, Coomassie brilliant blue. (D) In vitro pulldown assay using GST-fused nectin-2α C-term and MBP-fused PDZ domains of MUPP1 and Patj. The PDZ5 domain of MUPP1 and the PDZ5 domain of Patj specifically interacted with nectin-2α. (E) MUPP1-myc (b and c) or Patj-myc (d and e) was stably expressed in L cells that stably express nectin-2α (NL cells) (a, b, and d) or nectin-2αΔAVYV (NLΔAVYV cells) (c and e). Cells were then stained with anti-myc PAb and anti-nectin-2 MAb. As previously reported (48, 71), both nectin-2α and nectin-2αΔAVYV were concentrated at cell-cell contact sites (arrowheads). Nectin-2α, but not nectin-2αΔAVYV, recruited MUPP1 and Patj to these cell-cell contact sites. Bar, 10 μm.

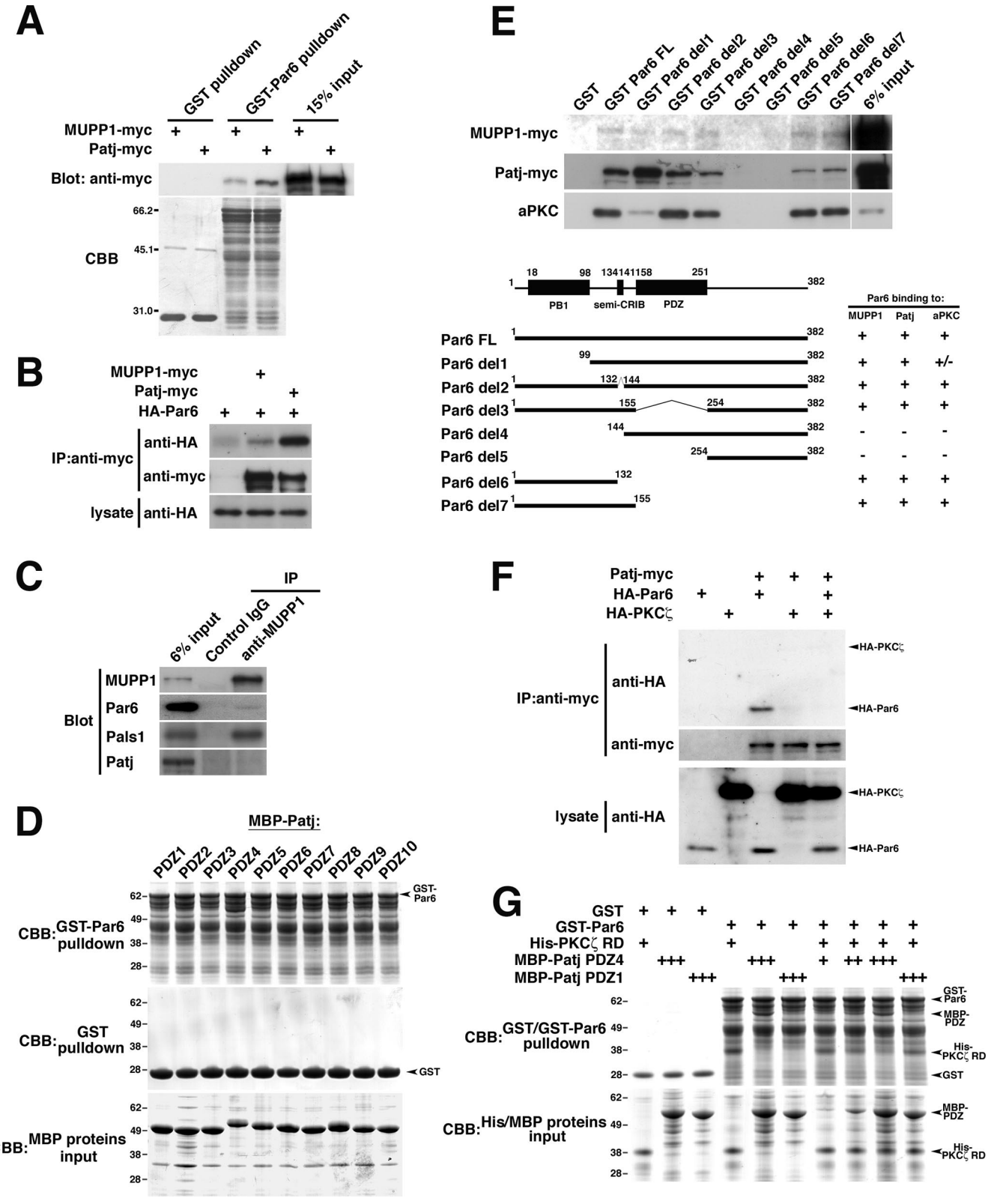

FIG. 5. Interaction with Par6. (A) In vitro pulldown assay using GST-Par6 (Par6A) and lysates of cells expressing MUPP1-myc or Patj-myc. Both MUPP1 and Patj interacted with Par6, but the interaction of MUPP1 was weaker than that of Patj. CBB, Coomassie brilliant blue. (B) Coimmunoprecipitation assay. MUPP1-myc or Patj-myc was coexpressed in HEK293 cells with HA-Par6 (Par6B). Cells were lysed and immunoprecipitated (IP) with anti-myc PAb, followed by immunoblotting with anti-HA MAb and anti-myc PAb. HA-Par6 was present in both MUPP1-myc and Patj-myc immunoprecipitates but was more abundant in the latter. (C) Immunoprecipitation of endogenous MUPP1 from EpH4 cells. Par6 (Par6B) and Pals1, but not Patj, coimmunoprecipitated with MUPP1. (D) In vitro pulldown assay using GST-Par6 (Par6A) and

domain of mouse nectin-1α (prey no. 99 [aa 381 to 515] and prey no. 456 [aa 389 to 515]) (Fig. 3A; see also Materials and Methods). A β-galactosidase assay confirmed the specific interaction of the cytoplasmic domain of nectin-1α with the PDZ2 domain, but not with other PDZ domains, of MUPP1 (Fig. 3B). Nectins have been well characterized as Ca^{2+}-independent cell adhesion molecules of AJs in epithelial cells (72). They comprise a gene family consisting of four members (nectin-1 to nectin-4), with two or three splicing variants for each, and, except for nectin-1β, -1γ, -3γ, and -4, have a PDZ-binding motif at their C terminus. Among them, nectin-2 is expressed abundantly in epithelial tissues, whereas nectin-1 is expressed mostly in the brain (72). We then found that nectin-2α, as well as nectin-1α, binds to both MUPP1 and Patj, whereas the affinity for Patj was significantly lower than that for MUPP1 (Fig. 3C). These interactions were dependent on their PDZ-binding motif (Fig. 3C), and the pulldown assay revealed that nectin-2α binds specifically to PDZ5 of MUPP1 and PDZ5 of Patj (Fig. 3D). This is consistent with the finding that PDZ2 and PDZ5 of MUPP1 are most similar to PDZ2 and PDZ5 of Patj, respectively. Also, the binding of nectin-1α and -2α to different PDZ domains of MUPP1 would be due to their distinct PDZ-binding motifs, EWYV and AVYV, respectively.

Because nectins and MUPP1 and Patj are respectively located at AJs and TJs in polarized epithelial cells, we examined whether their interactions actually occur within cells. First, we stably transfected MUPP1 and Patj into two types of L fibroblasts, NL and NLΔAVYV cells, which stably express nectin-2α and a PDZ-binding motif-deleted mutation (nectin-2αΔAVYV), respectively (48, 71). Both nectin-2α and nectin-2αΔAVYV were concentrated at cell-cell borders (Fig. 3E). MUPP1 and Patj were clearly recruited to the nectin-2α-based cell-cell contacts (Fig. 3E, panels b and d), whereas they were not apparent at the nectin-2αΔAVYV-based contacts but rather were distributed diffusely throughout the cytoplasm (Fig. 3E, panels c and e). Thus, nectin-2α is able to interact with MUPP1 and Patj within cells utilizing the PDZ-binding motif. Next, possible intracellular colocalization of nectin-2 and MUPP1 and Patj was examined. AJs and TJs are derived from common primordial junctional structures (spot-like AJs), which are sorted into epithelial junctions gradually as cellular polarization proceeds (4). When confluent EpH4 cell cultures were scratched with a needle, small E-cadherin-positive spot-like AJs formed between apposed cells of the wound 4 h later (data not shown). At that time point, nectin-2 appeared at these contacts as well (6), whereas MUPP1 and Patj were hardly detectable (see 4-h data in Fig. S1A and B in the supplemental material). These spot-like AJs began to align in a linear fashion (see 6-h data in Fig. S1A and B in the supplemental material) and grew to develop AJs and TJs at 8 h (see 8-h data in Fig. S1A and B in the supplemental material). We found that neither MUPP1 nor Patj was present at nectin-2-positive junctions at 4 h, but both proteins were detectable at 6 h, when TJs were not yet established (see Fig. S1A in the supplemental material). They then became concentrated at TJs at 8 h (see Fig. S1B in the supplemental material). Collectively, these data strongly suggested the occurrence of an interaction between nectin-2 and MUPP1 and Patj. It should also be noted that the behavior of MUPP1 was almost indistinguishable from that of Patj throughout these processes (see Fig. S1C in the supplemental material). Transient colocalization of nectin-2 and MUPP1 and Patj was also observed in F9 teratocarcinoma cells in the process of retinoic-acid-induced epithelial differentiation, during which junctions formed gradually (see Fig. S2 in the supplemental material).

Because nectins become apparent at primordial junctions earlier than MUPP1 and Patj and transiently colocalize with MUPP1 and Patj, they might be responsible for the recruitment of MUPP1 and Patj as junctions form. We then established EpH4 cells that stably express MUPP1Δ2,5-myc, which lacks the binding domains for nectin-1 and -2. When stably expressed in EpH4 cells, MUPP1Δ2,5 as well as full-length MUPP1 clearly localized to TJs and distributed to a slight extent in apical membranes and the cytoplasm in fully confluent cells, although the cytoplasmic vesicular distribution was more apparent for MUPP1Δ2,5 (Fig. 4A and data not shown). When examined 6 h after the wounding, MUPP1 was detectable at most nectin-2-positive primordial cell-cell junctions (Fig. 4B and C). By contrast, MUPP1Δ2,5 was apparent at only some nectin-2-positive junctions (Fig. 4B and C). Thus, nectins appear to be responsible for the junctional accumulation of MUPP1. Under the same conditions, the accumulation of MUPP1Δ2,3,4,5 was even more fractional (Fig. 4B and C), suggesting that another transmembrane protein that binds to PDZ3 of MUPP1, namely, JAM1, is responsible as well. Indeed, JAM1 is recruited to primordial junctions slightly later than nectin-2 but earlier than MUPP1 and Patj (data not shown). Nevertheless, it should be noted that other TJ proteins have also been shown to bind PDZ2 and -3 of MUPP1 (7, 25). Claudins are recruited later than MUPP1 and Patj, excluding their involvement in the junctional recruitment of MUPP1 and Patj (see Fig. S2 in the supplemental material and data not shown).

MBP-fused PDZ domains of Patj. GST-Par6 specifically interacted with MBP-PDZ4. GST did not interact with any of PDZ domains. (E) In vitro pulldown assays using several GST-fused deletion constructs of Par6 (Par6A) and lysates of cells exogenously expressing MUPP1-myc, Patj-myc, or nothing. Eluates were immunoblotted with anti-myc PAb and anti-aPKC PAb. The domain between PB1 and semi-CRIB of Par6 was involved in the interaction with MUPP1 and Patj. On the other hand, PB1 alone was necessary and sufficient for the interaction with aPKC. (F) Patj-myc was coexpressed in HEK293 cells with HA-Par6 (Par6B) and/or HA-PKCζ, as indicated, followed by immunoprecipitation with anti-myc PAb. PKCζ did not significantly coprecipitate with Patj but instead inhibited the interaction of Patj with Par6. (G) In vitro pulldown assays using different recombinant proteins. The His-PKCζ RD (containing the Par6-binding region), as well as MBP-Patj PDZ4, interacted with GST-Par6 (Par6A) but not with GST. Addition of increasing amounts of MBP-Patj PDZ4 to the reaction mixture accordingly inhibited the binding of His-PKCζ RD to GST-Par6. In a control experiment, MBP-Patj PDZ1 did not bind to GST-Par6 and had no effect on the Par6-PKCζ interaction. Note that in the coimmunoprecipitation assays whose results are presented in panels B and F, the Par6B isoform but not the Par6A isoform was used, but those two isoforms exhibit similar binding profiles with respect to MUPP1 and Patj (see Fig. S3 in the supplemental material).

Interaction with Par6. In *Drosophila* studies, Par6 has been reported to bind to Patj, although the occurrence of the interaction between their mammalian orthologues remains unclear (49, 79). We then carefully examined whether mammalian Par6 binds MUPP1 and Patj. In vitro pulldown assays revealed that Par6 binds to both MUPP1 and Patj, although its affinity for MUPP1 was significantly lower (Fig. 5A). Coimmunoprecipitation assays using HEK293 cells showed that Par6 coprecipitated with both MUPP1 and Patj; again, affinity was higher for Patj than for MUPP1 (Fig. 5B; see also Fig. S3A in the supplemental material). To address endogenous interaction, we immunoprecipitated MUPP1 from lysates of EpH4 cells and found that Par6 is present in the anti-MUPP1 immunoprecipitate (Fig. 5C). Collectively, these results suggest that interaction between mammalian MUPP1 and Patj and Par6 does occur both in vitro and in vivo. Although it is possible that Par6 interacts with MUPP1 and Patj via Pals1, which can interact with both MUPP1 and Patj and Par6 directly (22, 30, 58), that deletion of the Pals1-binding L27 domain of Patj did not affect the Par6-Patj interaction suggests that Pals1 does not have major roles in the Par6-Patj interaction, at least under our experimental conditions (see Fig. S3B in the supplemental material). In vitro pulldown assays revealed that PDZ4 of Patj is responsible for the binding (Fig. 5D), but we failed to determine the Par6-binding domain of MUPP1, probably due to the low affinity (data not shown). To identify the domain of Par6 interacting with MUPP1 and Patj, we tested several deletion constructs and found that the region between PB1 and semi-CRIB of Par6 is required for the interaction (Fig. 5E). Specifically, an aPKC-binding region of Par6 is located at PB1, just adjacent to the MUPP1 and Patj binding site (Fig. 5E) (35, 51, 55, 70), suggesting that the binding of aPKC to Par6 might have some effect on the binding of MUPP1 and Patj to Par6 and vice versa. We then found that coexpression of PKCζ severely impaired the interaction between Par6 and Patj (Fig. 5F). Note that we could not detect the interaction between aPKC and Patj, though interaction between their *Drosophila* orthologues has previously been demonstrated (64). Conversely, an excess amount of Patj inhibited the interaction between PKCζ and Par6 (Fig. 5G). These results suggest that the interactions of Par6 with Patj and aPKC are mutually exclusive.

Effects of dominant-negative constructs of MUPP1 and Patj. MUPP1 and Patj have several binding partners in common but do not necessarily share the same affinity for these partners, suggesting that they have their own unique functions. Thus, in an attempt to elucidate the roles of MUPP1 and Patj in the establishment of junctions, we overexpressed MUPP1 and Patj in EpH4 cells. When transiently transfected, both MUPP1 and Patj localized to TJs with a concomitant appearance in apical membranes and the cytoplasm, almost identical to the distribution of the respective endogenous proteins (Fig. 6A). Interestingly, in cells overexpressing MUPP1, the localization of endogenous Patj to TJs was almost completely abrogated (Fig. 6A, panel b, and D). In contrast, when Patj was overexpressed, the localization of endogenous MUPP1 to TJs was inhibited (Fig. 6A, panel d, and D). These results suggest that MUPP1 and Patj prevent endogenous Patj and MUPP1, respectively, from localizing to TJs by interacting with their shared TJ-anchoring proteins. Thus, MUPP1 and Patj have overlapping molecular characteristics in this respect. Importantly, in cells overexpressing MUPP1, when endogenous Patj was removed from TJs, the localization of Pals1 to TJs was severely impaired (Fig. 6A, panel c, and D). However, in cells expressing Patj, when MUPP1 was removed, Pals1 localized to TJs nearly normally (Fig. 6A, panel f, and D). These results suggest that, although MUPP1 and Patj both have the ability to bind Pals1, only Patj is required for the localization of Pals1 to TJs in vivo.

It has been reported that the transient transfection of the N terminus of Patj, which contains the L27 and PDZ1 domains, impaired the establishment of TJs in MDCKII cells (30, 58), probably because the L27 domain competitively inhibited the interaction between endogenous Pals1 and Patj. We then constructed similar dominant-negative constructs, MUPP1-L27 and Patj-L27, which contain solely the L27 domain of MUPP1 and Patj, respectively. In contrast to the full-length constructs, MUPP1-L27 or Patj-L27 mostly distributed diffusely in the cytoplasm, rather than being concentrated at cell-cell junctions (Fig. 6B). Importantly, the localization of both MUPP1 and Patj to TJs was severely inhibited by the expression of either L27 domain (Fig. 6B, panels a, b, d, and e, and D), and Pals1 was also removed from TJs in these cells (Fig. 6B, panels c and f, and D). This is consistent with reports that the localization of Pals1 to TJs is dependent on Patj (46, 58, 61). Also, both MUPP1-L27 and Patj-L27 inhibited the localization of Par6 and aPKC to TJs (Fig. 6C, panels a and b, and D). On the other hand, the localization of Par3 was only slightly affected (Fig. 6C, panel c, and D). These results suggest that the L27 domain alone is sufficient to exert dominant-negative effects and that the L27 domains of MUPP1 and Patj might have similar functions, at least when they are overexpressed.

Knockdown of MUPP1 and Patj by RNAi. To more directly address the functions of MUPP1 and Patj, we tried to knock down their expression by RNAi. Two distinct short interfering RNAs designed for MUPP1 (MUPP1 KD-1 and -2) and Patj (Patj KD-1 and -2) were stably expressed in EpH4 cells. In addition, two cell lines that stably coexpress MUPP1 KD-2 and Patj KD-1 as well as MUPP1 KD-2 and Patj KD-2 were also established (Fig. 7A). In all cases, expression of MUPP1 and Patj was suppressed by >90% (Fig. 7A and data not shown). Suppression of their expression was also confirmed by immunofluorescence microscopy (Fig. 7B). Significantly, TJs were significantly winding and fragmental in both Patj KD-1 and -2 cells, as revealed by staining with ZO-1 and claudin-3 (Fig. 7B and data not shown). This result is in line with reports that the knockdown of Patj in MDCKII cells or Caco2 cells resulted in defects in TJs (46, 61). Similar aberrant TJs were observed in MUPP1 KD-2 Patj KD-1 and MUPP1 KD-2 Patj KD-2 cells (Fig. 7B and data not shown). By contrast, TJs were normally established in MUPP1 KD-1 and -2 cells, as well as in control cells (Fig. 7B and data not shown). These results suggest that Patj, but not MUPP1, is specifically required for the establishment of TJs. Pals1 was almost completely absent from TJs in Patj KD cells but not in MUPP1 KD cells (Fig. 7C, panels a and f). This observation is consistent with the overexpression of MUPP1, which removed endogenous Patj from TJs, significantly inhibiting the localization of Pals1 to TJs (Fig. 6A, panel c), and confirms that Patj is specifically responsible for the normal localization of Pals1. Among components of the Par3-Par6-aPKC complex, localization of Par6 and aPKC was significantly impaired in Patj KD cells; only small quantities of

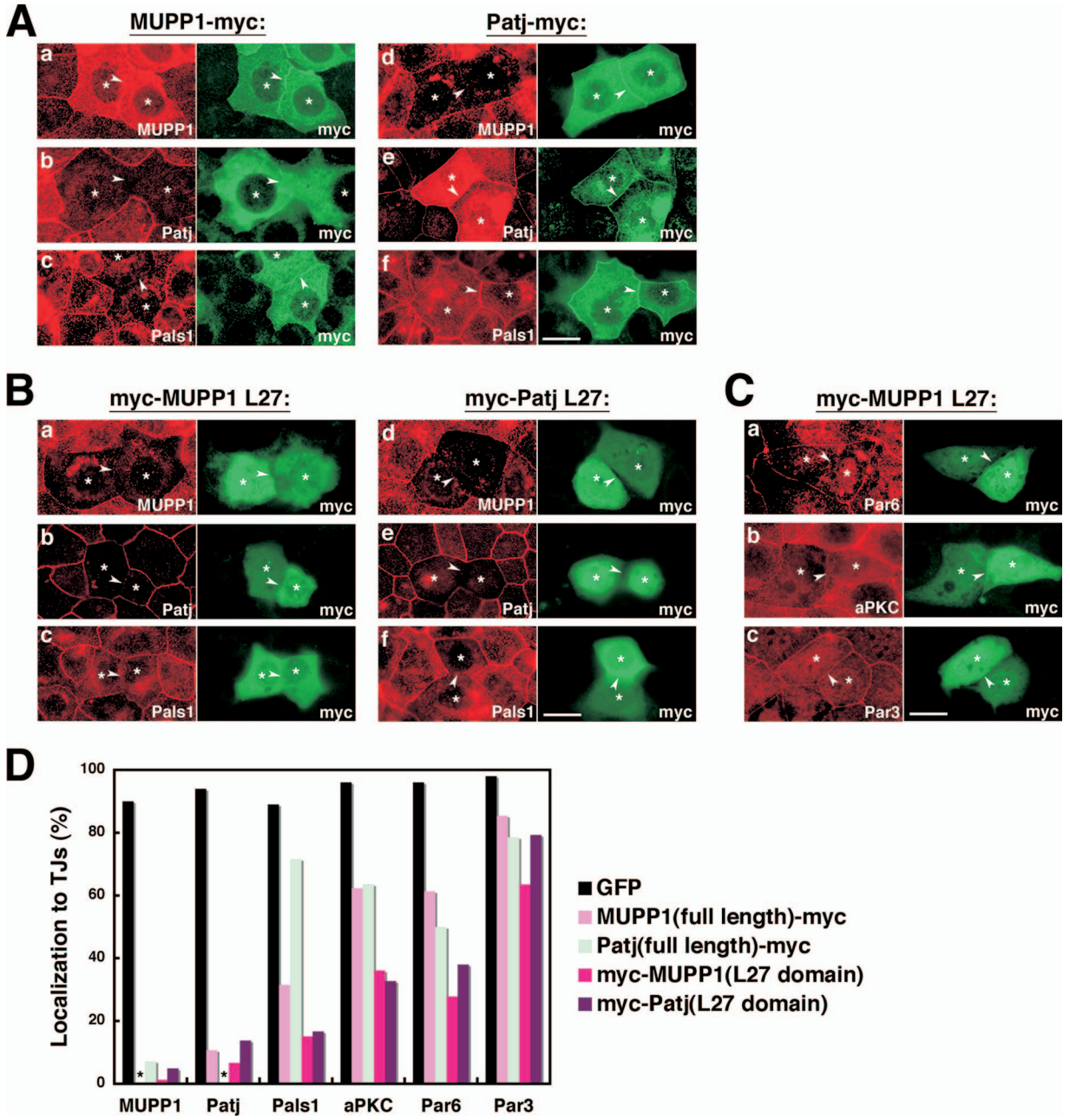

FIG. 6. Effects of expression of MUPP1 or Patj or their L27 domains. (A) EpH4 cells were transfected with MUPP1-myc (a, b, and c) or Patj-myc (d, e, and f) and stained with anti-MUPP1 MAb (a and d), anti-Patj PAb (b and e), or anti-Pals1 PAb (c and f). MUPP1-myc as well as Patj-myc localized to TJs, with a concomitant appearance at apical membranes and in the cytoplasm. (b) At TJs between cells expressing MUPP1-myc, localization of endogenous Patj to TJs was inhibited. (d) On the other hand, expression of Patj-myc inhibited the localization of endogenous MUPP1. Localization of Pals1 was evidently inhibited by expression of MUPP1-myc (c) but not by expression of Patj-myc (f). (B) EpH4 cells were transfected with myc-MUPP1-L27 (a, b, and c) or myc-Patj-L27 (d, e, and f) and stained as described for panel A. Both myc-MUPP1-L27 and myc-Patj-L27 distributed mostly in the cytoplasm and similarly abrogated the localization of endogenous MUPP1, Patj, and Pals1 to TJs. (C) EpH4 cells were transfected with myc-MUPP1-L27 and stained with anti-Par6 PAb (a), anti-aPKC PAb (b), or anti-Par3 PAb (c). Localization of Par6 and aPKC was severely impaired, whereas that of Par3 was mostly normal at TJs between cells expressing myc-MUPP1-L27. In panels A to C, asterisks indicate cells expressing the myc constructs, and arrowheads point to the locations of cell-cell junctions between them. Bars, 10 μm. (D) Quantification of the results shown in panels A to C. Percentages of cell-cell junctions where junctional proteins were appropriately targeted were calculated for each set of conditions. Note that the localization of endogenous MUPP1 and Patj could not be examined when full-length MUPP1-myc and Patj-myc were expressed, respectively (asterisks). A total of 52 to 149 cell-cell junctions were examined for each set of conditions. GFP, green fluorescent protein.

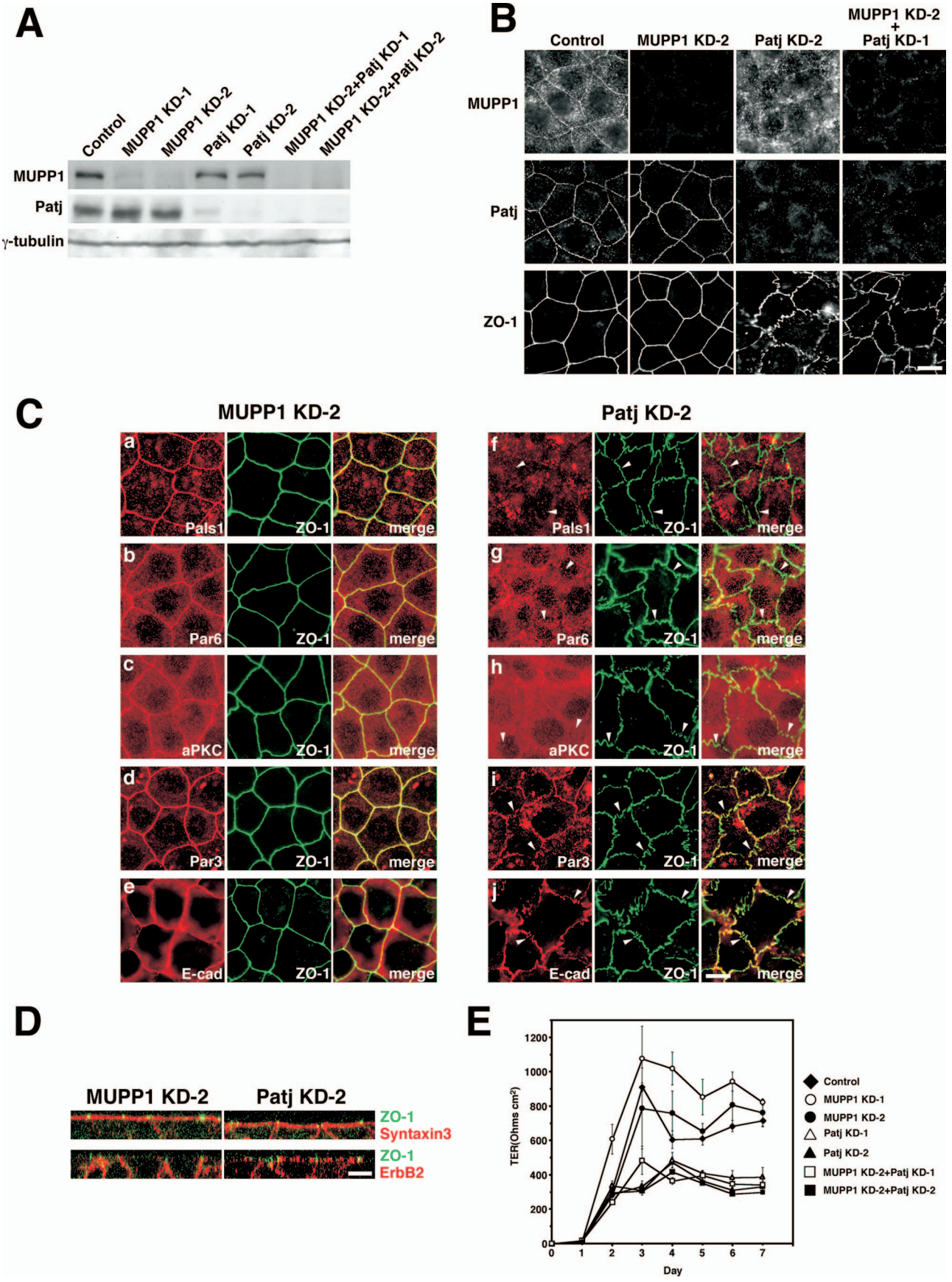
A
Control
MUPP1 KD-1
MUPP1 KD-2
Patj KD-1
Patj KD-2
MUPP1 KD-2+Patj KD-1
MUPP1 KD-2+Patj KD-2
MUPP1
Patj
γ-tubulin
B
Control
MUPP1 KD-2
Patj KD-2
MUPP1 KD-2 + Patj KD-1
MUPP1
Patj
ZO-1
C
MUPP1 KD-2
Patj KD-2
a
Pals1
ZO-1
merge
b
Par6
c
aPKC
d
Par3
e
E-cad
f
g
h
i
j
D
MUPP1 KD-2
Patj KD-2
ZO-1
Syntaxin3
ErbB2
E
TER(Ohms cm²)
Day
Control
MUPP1 KD-1
MUPP1 KD-2
Patj KD-1
Patj KD-2
MUPP1 KD-2+Patj KD-1
MUPP1 KD-2+Patj KD-2

Par6 and aPKC were detected in ZO-1-positive regions, and most was located in the cytoplasm (Fig. 7C, panels b, c, g, and h). On the other hand, Par3 remained mostly colocalized with ZO-1 at the fragmental junctions (Fig. 7C, panels d and i). Thus, Par3 was affected differently from Par6 and aPKC by the knockdown of Patj, consistent with the effects of dominant-negative constructs (Fig. 6C and D). In Patj KD cells, AJs were also severely affected, as revealed by immunostaining of AJ-associated proteins, including E-cadherin, α-catenin, nectin-2, and afadin, all of which mostly colocalized with ZO-1 (Fig. 7C, panels e and j, and data not shown).

In both wild-type and MUPP1 KD cells grown on Transwell filters, syntaxin 3 (an apical marker) and ErbB2 (a lateral marker) (76) were normally distributed, with their apical and lateral localizations clearly compartmentalized at ZO-1-positive TJs, respectively, as shown by confocal microscopy (Fig. 7D and data not shown). In Patj KD cells and MUPP1 KD Patj KD cells, however, these marker proteins leaked out of their original compartments in significant quantities and became detectable at both apical and lateral membranes (Fig. 7D and data not shown). Thus, Patj, but not MUPP1, is required for the fence function of TJs. To examine the barrier function, we measured TER. In MUPP1 KD cells, TER gradually increased to almost the levels seen in wild-type cells as cells reached confluence after reseeding (Fig. 7E). By contrast, in Patj KD cells, the increase was only slight; at Day 7, the value was approximately half that seen with wild-type or MUPP1 KD cells (Fig. 7E). Importantly, the TER value of MUPP1 Patj KD cells was almost indistinguishable from that of Patj KD cells (Fig. 7E). These results suggest that Patj is specifically involved in the establishment of the barrier function of TJs whereas MUPP1 is not.

Although the loss of MUPP1 apparently did not affect the integrity of TJs, many proteins do not affect the steady-state structure of TJs in polarized cells but affect the process of its establishment. Thus, we performed a Ca^{2+}-switch assay. In this assay, cells were cultured in a low-Ca^{2+} medium containing 5 μM of Ca^{2+} overnight and were then transferred to a normal medium to initiate the polarization of cells ("Ca^{2+} switch"). In wild-type cells, the ZO-1-positive TJs were gradually reformed after the Ca^{2+}-switch and were almost completely established at 2 h (Fig. 8A). Significantly, the time courses of the establishment of TJs were indistinguishable between wild-type cells and MUPP1 KD cells (Fig. 8A). On the other hand, in both Patj KD and MUPP1 KD Patj KD cells, the formation of TJs was severely retarded and was only partially completed at 2 h. Therefore, MUPP1 is dispensable not only for the steady-state structure of TJs but also for the process of their establishment, whereas Patj is required for both. Similarly, AJs were normally established in MUPP1 KD cells, as revealed by nectin-2 staining, whereas they were present only in premature form in Patj KD and MUPP1 KD Patj KD cells (Fig. 8B).

Molecular background of phenotypes of Patj KD cells. We then examined the effect of restoring the expression of MUPP1 and Patj in MUPP1 KD Patj KD cells by re-expressing RNAi-resistant constructs. Restoring the expression of MUPP1 had no effect on the integrity of TJs (Fig. 9A, panels a and g), which is in line with the absence of Patj alone resulting in aberrant TJs (Fig. 7). By contrast, expression of Patj resulted in the establishment of linear TJ strands and concomitantly rescued the localization of Pals1 to TJs (Fig. 9A, panels b and h). This result confirms that the phenotypes of Patj KD cells were not due to the nonspecific effect of RNAi. Significantly, expression of PatjΔL27, which lacks the L27 domain, was by no means effective; although PatjΔL27 colocalized with ZO-1 at premature junctions, these junctions were only fragmentary, as was seen in parental MUPP1 KD Patj KD cells, and neither Pals1 nor Par6 was colocalized (Fig. 9A, panels c and i, and data not shown). PatjΔ4, in which PDZ4 was deleted, on the other hand, successfully restored TJs as efficiently as full-length Patj did, and Par6, as well as Pals1, was normally localized to TJs (Fig. 8A, panels d and j, and data not shown). These results suggest that the interaction with Pals1 is absolutely critical for Patj to exert its function and that the interaction with Par6 is not necessarily functionally significant. We then tested PatjΔ2,5 (because PDZ2 and -5 are probable binding sites for nectins) and found that it was sufficient for the formation of AJs and TJs (Fig. 9A, panels e and k, and data not shown). We have also tested Patj-L27, which does not possess any PDZ domains but does possess an L27 domain. Significantly, Patj-L27 distributed throughout the cytoplasm and was absolutely inactive (Fig. 9A, panels f and l). Thus, the L27 domain of Patj, though sufficient for interaction with Pals1, is not sufficient for the establishment of TJs. Interactions via PDZ domains are evidently essential.

It has been hypothesized that Pals1 is responsible for the assembly of TJs, because it recruits and activates the Par6-aPKC complex at TJs (66). We have found that the knockdown of Patj but not of MUPP1 specifically resulted in the loss of Pals1, as well as Par6 and aPKC, from TJs and that the re-

FIG. 7. Knockdown of MUPP1 and Patj by RNAi. (A) Immunoblotting with anti-MUPP1 MAb and anti-Patj PAb of lysates of control, two MUPP1 RNAi (MUPP1 KD-1 and MUPP1 KD-2), two Patj RNAi (Patj KD-1 and Patj KD-2), and two MUPP1 and Patj RNAi (MUPP1 KD-2 Patj KD-1 and MUPP1 KD-2 Patj KD-2) stable EpH4 cell lines. Blotting for γ-tubulin was used as a loading control. (B) Control, MUPP1 KD-2, Patj KD-2, and MUPP1 KD-2 Patj KD-1 cells were grown to confluence on glass coverslips and stained with anti-MUPP1 MAb, anti-Patj PAb, or anti-ZO-1 MAb. TJs were linearly established in control and MUPP1 KD-2 cells, whereas they were fragmentary in Patj KD-2 cells and MUPP1 KD-2 Patj KD-1 cells. Bar, 10 μm. (C) MUPP1 KD-2 and Patj KD-2 cells were stained with anti-Pals1 PAb (a and f), anti-Par6 PAb (b and g), anti-aPKC PAb (c and h), anti-Par3 PAb (d and i), and anti-E-cadherin MAb (e and j). In MUPP1 KD-2 cells, the localization of these junctional proteins was normal (a to e). In Patj KD cells, Pals1, Par6, and aPKC were severely delocalized from ZO-1-positive fragmental junctions, whereas Par3 and E-cadherin mostly colocalized with ZO-1 (arrowheads). Bar, 10 μm. (D) MUPP1 KD-2 and Patj KD-2 cells were grown on Transwell filters and stained with anti-ZO-1 MAb (green) and anti-Syntaxin3 PAb (red) (upper panels) and with anti-ZO-1 MAb (green) and anti-ErbB2 PAb (red) (lower panels). Vertical sectional images were generated by confocal microscopy. In MUPP1 KD-2 cells, Syntaxin3 and ErbB2 localized to apical membranes and lateral membranes, respectively, whereas in Patj KD-2 cells, they were localized to both apical and lateral membranes. Bar, 10 μm. (E) TER of control, MUPP1 KD-1, MUPP1 KD-2, Patj KD-1, Patj KD-2, MUPP1 KD-2 Patj KD-1, and MUPP1 KD-2 Patj KD-2 cells. The knockdown of Patj significantly affected the development of the epithelial barrier ($n = 4$ for each cell line).

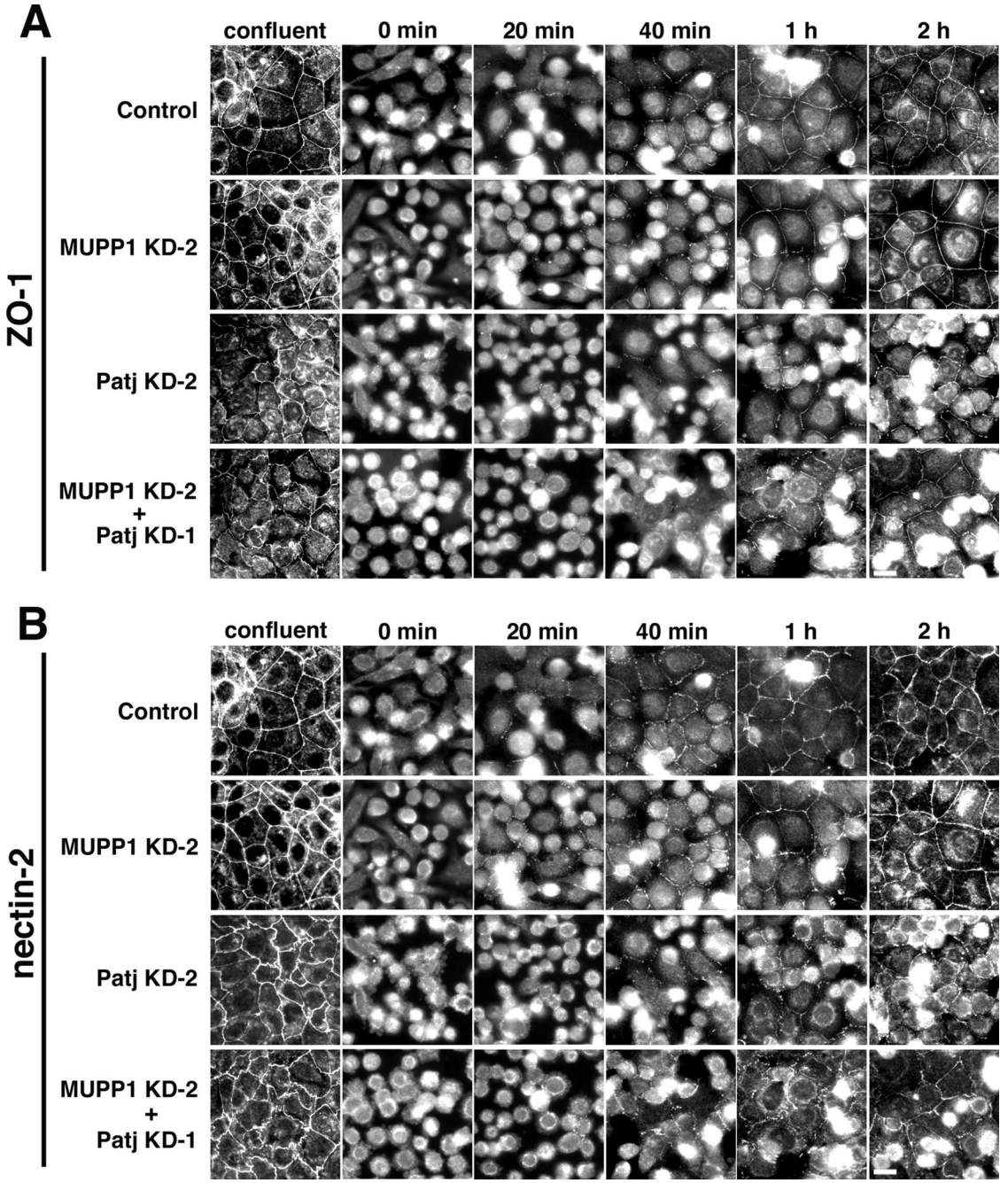

FIG. 8. Ca^{2+}-switch assay. Control, MUPP1 KD-2, Patj KD-2, and MUPP1 KD-2 Patj KD-1 cells were grown to confluence on glass coverslips. They were then transferred to a low-Ca^{2+} medium overnight to disassemble the junctions and returned to normal culture medium. At different time points after the addition of the medium, cells were fixed and stained with anti-ZO-1 PAb (A) and anti-nectin-2 MAb (B). Formation of ZO-1-positive TJs as well as nectin-2-positive AJs was severely retarded by the knockdown of Patj. Bar, 10 μm.

cruitment of Pals1 to TJs was principally responsible for the function of Patj. Thus, it is suggested that the morphological defects of TJs in Patj KD cells might be reversed by forced junctional recruitment of the active Par6-aPKC complex. To test this assumption, we transfected Patj KD cells with a constitutively active form of Cdc42 (Cdc42G12V) that can interact with and activate this complex directly (80). Significantly, we found that linear TJ-like junctions were clearly established between the cells expressing Cdc42G12V, as revealed by staining of ZO-1, Pals1, and claudin-3 (Fig. 9B, panels a and c; see also Fig. S4 in the supplemental material). Thus, Cdc42G12V can rescue the accumulation of TJ components to cell-cell junctions. When examined by confocal microscopy, however, these junctions were not concentrated apically in lateral cell membranes but extended laterally throughout, and they clearly colocalized with overexpressed Cdc42G12V at

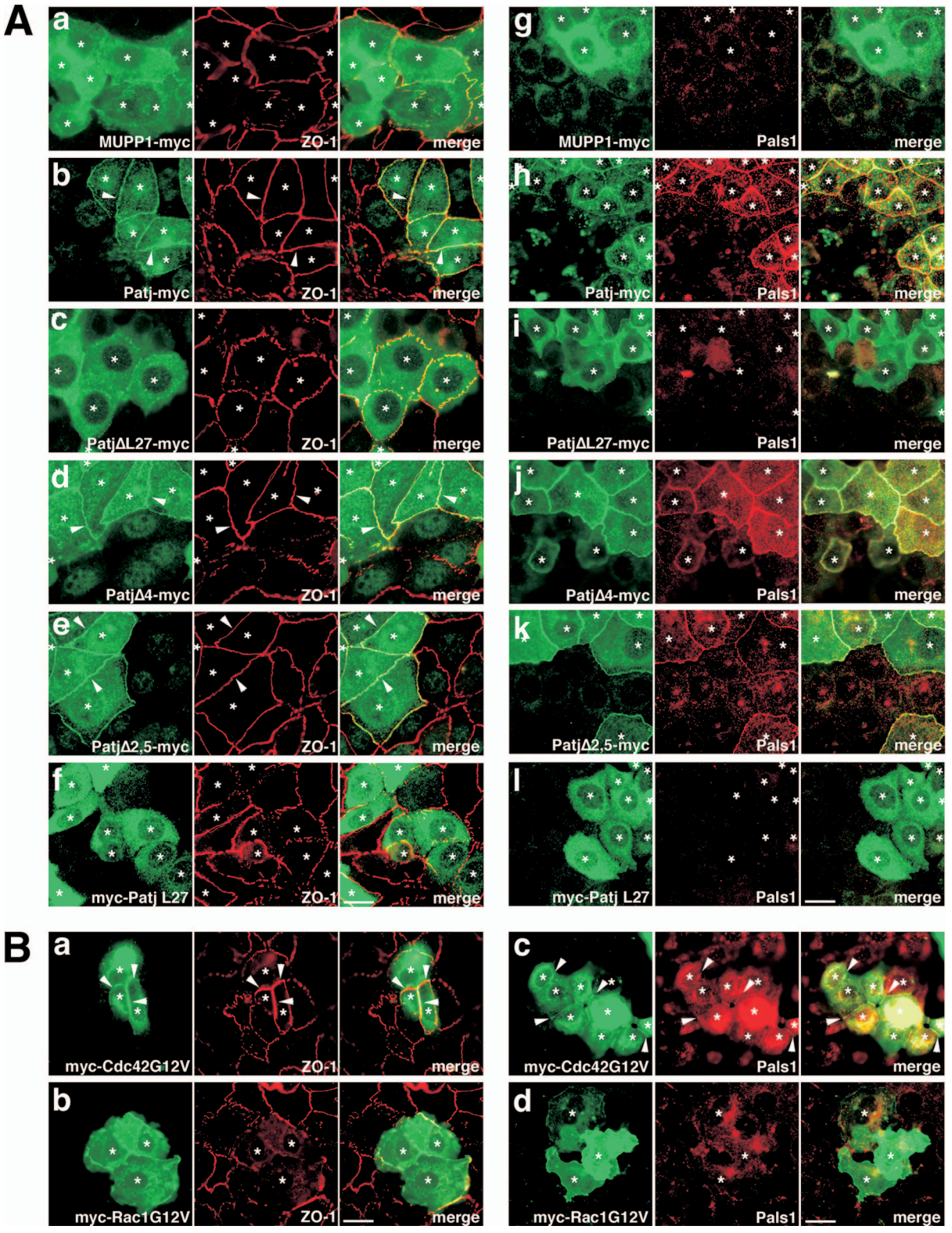

FIG. 9. Attempts to rescue aberrant TJs in Patj KD cells. (A) MUPP1 KD-2+Patj KD-1 cells were stably transfected with MUPP1-myc (a and g), Patj-myc (b and h), PatjΔL27-myc (c and i), PatjΔ4-myc (d and j), PatjΔ2,5-myc (e and k), and myc-Patj L27 (f and l) and stained with anti-ZO-1 PAb (a to f) or anti-Pals1 PAb (g to l). The expression levels of the constructs were similar (data not shown). Expression of Patj, PatjΔ4, and PatjΔ2,5 restored the development of linear TJs (b, d, and e [arrowheads]), whereas that of MUPP1, PatjΔL27, and Patj L27 was ineffective (a, c, and f). Expression of Patj, PatjΔ4, and PatjΔ2,5 also restored the junctional localization of Pals1 (h, j, and k), but that of MUPP1, PatjΔL27, and Patj L27 did not (g, i, and l). Note that except for Patj-L27, which does not cover the targeted region of RNAi, point mutations were introduced into all Patj constructs to attain RNAi resistance. Asterisks indicate cells expressing the myc constructs. Bars, 10 μm. (B) Patj KD-1 cells were transfected with myc-Cdc42G12V (a and c) or myc-Rac1G12V (b and d) and stained with anti-ZO-1 MAb (a and b) or anti-Pals1 PAb (c and d). Expression of Cdc42G12V restored the junctional accumulation of ZO-1 and Pals1 in a linear fashion (a and c [arrowheads]). By contrast, Rac1G12V was ineffective (b and d). Asterisks indicate cells expressing the myc constructs. Bars, 10 μm.

these lateral membranes (see Fig. S4 in the supplemental material). Thus, apicobasal cell polarity was not properly recaptured by the overexpression of Cdc42G12V. On the other hand, the active form of Rac1 (Rac1G12V) was unable to exert this effect, suggesting a functional divergence of small GTPases (Fig. 9B, panels b and d). Collectively, these results strongly suggest that the occurrence of abnormal TJs in Patj KD cells can be explained at least in part by the loss of Pals1-mediated activation of the Par6-aPKC complex in these premature junctions.

DISCUSSION

In this study, we examined the molecular properties and functions of MUPP1 and Patj in epithelial cells. Significantly, Patj was indispensable for epithelial polarization and the formation of TJs, but MUPP1 was not. This result was surprising, because the two proteins have several similarities: (i) they have highly homologous molecular structures; (ii) according to the public EST database, their expression overlaps in many tissues (data not shown); (iii) they have the ability to interact with several common junction-associated proteins; (iv) they both localize to TJs and apical membranes in polarized epithelial cells; (v) the rates at which they accumulate at TJs in the process of epithelial polarization are almost identical; and (vi) overexpression of MUPP1 and Patj removes endogenous Patj and MUPP1 from TJs, respectively, suggesting that they utilize overlapping molecular mechanisms to localize to TJs. Even so, we found several individual characteristics of MUPP1 and Patj. Most importantly, they differ in their levels of affinity for the binding partners they share. Thus, the functional discrepancy between MUPP1 and Patj is most likely due to the differences in affinity shown by these proteins.

In this study, the affinities for JAM1 and ZO-3 did not differ markedly between MUPP1 and Patj. Both JAM1 and ZO-3 clearly localized to ZO-1-positive cell-cell junctions in Patj-KD cells or cells expressing dominant-negative MUPP1 and Patj (data not shown). Thus, MUPP1 and Patj are not directly responsible for their localization to TJs. Rather, MUPP1 and Patj might be recruited to TJs via an interaction with JAM1. In fact, we have found that both MUPP1 and Patj were recruited to JAM1-based cell-cell adhesion sites in L cells that stably express JAM1, which demonstrates that JAM1 is capable of accumulating MUPP1 and Patj at JAM1-positive cell-cell adhesion sites (data not shown). This idea is also in line with JAM1 being responsible for the junctional recruitment of another PDZ domain-containing protein, namely, Par3 (15, 33). On the other hand, the physiological significance of the interaction between MUPP1 and Patj and ZO-3 is unclear; although ZO-3 is reportedly required for the localization of Patj to TJs, because deletion of the ZO-3-binding domain (PDZ6) inhibited the localization of Patj to TJs (57), both MUPP1 and Patj normally localized to TJs in ZO-3-deficient mice and cultured cells (2). The use of different sets of experimental conditions might be the reason for this inconsistency. Alternatively, PDZ6 of Patj (corresponding to PDZ7 of MUPP1) might have unknown binding partners that are responsible for the recruitment of Patj to TJs. It must be mentioned that, utilizing in vitro pulldown assays, we have previously shown that JAM1 binds to PDZ9 of MUPP1 (27). In the present study, however, we found that JAM1 binds to PDZ3 of MUPP1 and to PDZ3 of Patj, utilizing similar methodologies (Fig. 2B). The reason for this discrepancy is probably that we previously used an inappropriate recombinant JAM1 protein that is highly insoluble when expressed in normal *E. coli* strains. In the present study, we used an *E. coli* strain that expresses a sort of chaperone, which improved the solubility and quality of the proteins expressed. Thus, we believe that the new data are more reliable. The fact that both MUPP1 and Patj can bind to JAM1 whereas Patj does not harbor the domain that corresponds to PDZ9 of MUPP1 is consistent with the notion that PDZ9 of MUPP1 is not actually responsible for the binding. PDZ3 of MUPP1 corresponds to PDZ3 of Patj, supporting the idea that these domains are more likely binding sites for JAM1.

Here we identified nectins as the first AJ proteins to be shown to interact with MUPP1 and Patj. In addition, nectins are shown to be responsible for effective junctional recruitment of MUPP1 and, possibly, of Patj. The issue, then, is whether their interactions are functionally significant with respect to the formation of junctions. AJs and TJs are known to be significantly associated functionally. It has been reported that the establishment of TJs is dependent on the integrity of AJs (52). In fact, nectins have an ability to establish TJs by themselves by binding, directly or indirectly, to several junction-associated peripheral membrane proteins (72). Therefore, it is possible that MUPP1 and Patj is involved in the nectin-dependent formation of TJs. We have found, however, that Patj lacking binding sites for nectins could successfully rescue the defects in AJs and TJs in Patj KD cells. Therefore, it seems unlikely that the interaction of nectins with MUPP1 and Patj is crucial to their functions. This might be consistent with the finding that MUPP1, whose knockdown apparently exerted no significant cellular defects, preferred to interact with nectins rather than with Patj. Even so, however, these interactions might well have accessory roles, with nectins reinforcing the formation of TJs by binding to MUPP1 and Patj, which in turn are responsible for the recruitment of several other junctional proteins.

Because Patj but not MUPP1 was specifically responsible for the establishment of cell-cell junctions, that Pals1 and Par6 preferentially bound to Patj strongly suggests that these two proteins are key to explaining the functions of Patj. Actually, Patj is responsible for their localization, because knockdown of Patj or inhibition of the junctional localization of Patj by dominant-negative Patj severely delocalized Pals1 and Par6 from TJs. Nevertheless, we also found that removal of the Par6-binding region from Patj apparently did not impair the ability of Patj to recruit Par6 as well as Pals1 to TJs or to establish cell polarity. Thus, the significance of the direct interaction between Patj and Par6 is not clear at present. However, we speculate that their interaction is potentially functional. Because Pals1 regulates the junctional accumulation of Par6 through direct interaction and because the localization of Pals1 is dependent on Patj, it is possible that Patj has a role in the localization of Par6 via Pals1. Then the direct interaction of Patj with Par6 might well have a complementary role in the correct junctional accumulation of Par6. In agreement with this, MUPP1 and Patj and Par6 accumulated at cell-cell junctions almost concurrently (data not shown). We also found that

the interaction between Patj and Par6 and that between Par6 and aPKC are mutually exclusive. It is known that Par6 modulates the activity of aPKC either positively or negatively, depending on its association with or dissociation from small GTPases (80). Then it is possible that Patj (and possibly MUPP1) regulates the formation of the Par6-aPKC complex so that the activity of aPKC is appropriately provided during the formation of junctions. This sort of regulation might be important for fine tuning or elaborate temporal and spatial regulation of aPKC kinase activity within cells. It should be noted that the targeting and activity of Par6 is regulated even more intricately; the interaction between Par6 and Pals1 is competitively inhibited by the interaction between Patj and Pals1 (79). In addition, both Par6 and Pals1 interact with the cytoplasmic PDZ-binding motif of Crb3, suggesting that Par6 and Pals1 share the same mechanisms to localize to TJs (41).

Nonetheless, Pals1 seems to be of primary importance to the function of Patj, because deletion of the Pals1-binding region severely impaired Patj's function. As mentioned above, one of the most important functions of Pals1 is to recruit the Par6-aPKC complex to TJs. Thus, the Pals1-mediated junctional localization of this complex might well be important to Patj's function. We confirmed this assumption by showing that expression of Cdc42G12V, which forcibly activates this complex, rescued the junctional accumulation of molecular components of TJs in Patj KD cells. Moreover, the aberrant premature junctions apparent in Patj KD cells were quite similar to those found in cells that overexpress dominant-negative aPKC (68, 70). Thus, we speculate that the defects found in Patj KD cells are partly due to the aberrant regulation of the Par6-aPKC complex. Nevertheless, that Rac1G12V, which similarly interacts with this complex at least in vitro (35, 42, 51, 55), was unable to rescue Patj KD cells suggests that the effect of Cdc42G12V is not simply mediated by the Par6-aPKC pathway but might also involve the activation of other pathways (17), which are potentially regulated by Patj under normal conditions.

In *Drosophila* flies, Patj plays a critical role in photoreceptor morphogenesis, and this effect is mostly mediated by its N-terminal region containing the L27 and PDZ1 domains, whereas the C-terminal region containing the PDZ2 to -4 domains appears to have comparatively minor roles (50). This result is consistent with our observation that the L27 domain has prominent roles in Patj's function. Nevertheless, because in our experiments, the L27 domain alone was unable to rescue aberrant TJs in Patj KD cells, it is speculated that one of the functions of PDZ domains is to adequately localize the L27 domain to TJs. In this regard, a recent report has shown that Patj is involved in the directional migration of epithelial cells, for which the L27, PDZ1 to -5, and PDZ6 to -10 domains were comparably important (62). Thus, it is interesting to speculate that Patj might utilize different molecular mechanisms in directional migration and apicobasal polarization of epithelial cells.

In previous reports, knockdown of Patj in MDCKII cells led to defects in the formation of TJs and cell polarization (61), whereas in Caco2 cells, delocalization of some components such as occludin and Crb3 occurred but the overall structure of TJs was preserved (46). Given our observations of EpH4 cells, this phenotypic discrepancy would seem to be due to the use of different cell lines or experimental conditions. Despite some differences, however, it seems certain that Patj has important functions. On the other hand, we could not find any significant functions of MUPP1. Lanaspa et al. (38) recently reported that knockdown of MUPP1 resulted in a marked loss of TER in mouse inner medullary collecting duct IMCD3 cells, suggesting that MUPP1 is involved in maintaining the integrity of TJs (38). Although it is possible that we have overlooked MUPP1's functions because our RNAi constructs were not sufficiently effective, we speculate that the use of different cell lines more likely explains this discrepancy. Indeed, although MUPP1 was exclusively localized to TJs and apical membranes in EpH4 cells, it was distributed throughout lateral membranes in IMCD3 cells (38). Other than its expression in epithelial cells, MUPP1 is expressed abundantly in several nonepithelial tissues such as photoreceptor cells, neurons, and spermatozoa, where several binding partners for MUPP1 were previously identified (1, 8, 16, 37, 77). Thus, it is possible that MUPP1 is functionally significant in these cells, but clarification of this speculation awaits further investigation.

In summary, we found that MUPP1 and Patj in common interact with multiple molecules believed to be involved in regulating the assembly of TJs and epithelial polarity. However, Patj but not MUPP1 is specifically responsible for these processes. That several regulatory molecules differ in their affinities for MUPP1 and Patj might well be the reason for these functional differences. Notably, Pals1 seem to be the key to explaining the functional predominance of Patj in epithelial cells. To better clarify the possible functions of MUPP1, further investigation will be needed, including the generation of knockout mice.

ACKNOWLEDGMENTS

We thank Y. Takai, H. Nakanishi, A. Le Bivic, S. Ohno, E. Reichmann, and J. Behrens for providing materials. We also thank all the members of Tsukita laboratory (Department of Cell Biology, Faculty of Medicine, Kyoto University) for discussions. Our thanks are also due to Senye Takahashi for anti-Pals1 antiserum, Orie Koga for technical assistance, and Eisuke Nishida for allowing us to use equipment.

This study was supported in part by a Grant-in-Aid for Cancer Research (to Shoichiro Tsukita and Mikio Furuse), a Grant-in-Aid for Young Scientists (B) (to Makoto Adachi) and a Grant-in-Aid for Scientific Research (A) (to Shoichiro Tsukita) from the Ministry of Education, Culture, Sports, Science and Technology of Japan.

REFERENCES

1. **Ackermann, F., N. Zitranski, D. Heydecke, B. Wilhelm, T. Gudermann, and I. Boekhoff.** 2008. The Multi-PDZ domain protein MUPP1 as a lipid raft-associated scaffolding protein controlling the acrosome reaction in mammalian spermatozoa. J. Cell. Physiol. **214:**757–768.
2. **Adachi, M., A. Inoko, M. Hata, K. Furuse, K. Umeda, M. Itoh, and S. Tsukita.** 2006. Normal establishment of epithelial tight junctions in mice and cultured cells lacking expression of ZO-3, a tight junction MAGUK protein. Mol. Cell. Biol. **26:**9003–9015.
3. **Anderson, J. M., and C. M. Van Itallie.** 1995. Tight junctions and the molecular basis for regulation of paracellular permeability. Am. J. Physiol. **269:**G467–G475.
4. **Ando-Akatsuka, Y., S. Yonemura, M. Itoh, M. Furuse, and S. Tsukita.** 1999. Differential behavior of E-cadherin and occludin in their colocalization with ZO-1 during the establishment of epithelial cell polarity. J. Cell. Physiol. **179:**115–125.
5. **Aoki, J., S. Koike, H. Asou, I. Ise, H. Suwa, T. Tanaka, M. Miyasaka, and A. Nomoto.** 1997. Mouse homolog of poliovirus receptor-related gene 2 product, mPRR2, mediates homophilic cell aggregation. Exp. Cell Res. **235:**374–384.
6. **Asakura, T., H. Nakanishi, T. Sakasaka, K. Takahashi, K. Mandai, M. Nishimura, T. Sasaki, and Y. Takai.** 1999. Similar and differential behavior between the nectin-afadin-ponsin and cadherin-catenin systems during the formation and disruption of the polarized junctional alignment in epithelial cells. Genes Cells **4:**573–581.

7. **Assémat, E., E. Bazellières, E. Pallesi-Pocachard, A. Le Bivic, and D. Massey-Harroche.** 2008. Polarity complex proteins. Biochim. Biophys. Acta **1778:** 614–630.
8. **Balasubramanian, S., S. R. Fam, and R. A. Hall.** 2007. GABAB receptor association with the PDZ scaffold Mupp1 alters receptor stability and function. J. Biol. Chem. **282:**4162–4171.
9. **Barritt, D. S., M. T. Pearn, A.H. Zisch, S.S. Lee, R.T. Javier, E.B. Pasquale, and W. B. Stallcup.** 2000. The multi-PDZ domain protein MUPP1 is a cytoplasmic ligand for the membrane-spanning proteoglycan NG2. J. Cell. Biochem. **79:**213–224.
10. **Bhat, M. A., S. Izaddoost, Y. Liu, K.O. Cho, K.W. Choi, and H. J. Bellen.** 1999. Discs lost, a novel multi-PDZ domain protein, establishes and maintains epithelial polarity. Cell **96:**833–845.
11. **Bilder, D., M. Schober, and N. Perrimon.** 2003. Integrated activity of PDZ protein complexes regulates epithelial polarity. Nat. Cell Biol. **5:**53–58.
12. **Brummelkamp, T. R., R. Bernards, and R. Agami.** 2002. A system for stable expression of short interfering RNAs in mammalian cells. Science **296:**550–553.
13. **Cohen, C. J., J. Y. Shieh, R.J. Pickles, T. Okegawa, J. T. Hsieh, and J. M. Bergelson.** 2001. The coxsackievirus and adenovirus receptor is a transmembrane component of the tight junction. Proc. Natl. Acad. Sci. USA **98:**15191–15196.
14. **Ebnet, K.** 2008. Organization of multiprotein complexes at cell-cell junctions. Histochem. Cell Biol. **130:**1–120.
15. **Ebnet, K., A. Suzuki, Y. Horikoshi, T. Hirose, M. K. Meyer zu Brickwedde, S. Ohno, and D. Vestweber.** 2001. The cell polarity protein ASIP/PAR-3 directly associates with junctional adhesion molecule (JAM). EMBO J. **20:** 3738–3748.
16. **Estévez, M. A., J. A. Henderson, D. Ahn, X.R. Zhu, G. Poschmann, H. Lübbert, R. Marx, and J. M. Baraban.** 2008. The neuronal RhoA GEF, Tech, interacts with the synaptic multi-PDZ-domain containing protein, MUPP1. J. Neurochem. **106:**1287–1297.
17. **Etienne-Manneville, S.** 2004. Cdc42—the centre of polarity. J. Cell Sci. **117:**1291–1300.
18. **Etienne-Manneville, S., and A. Hall.** 2003. Cell polarity: Par6, aPKC and cytoskeletal crosstalk. Curr. Opin. Cell Biol. **15:**67–72.
19. **Farquhar, M. G., and G. E. Palade.** 1963. Junctional complexes in various epithelia. J. Cell Biol. **17:**375–412.
20. **Furuse, M., K. Fujita, T. Hiiragi, K. Fujimoto, and S. Tsukita.** 1998. Claudin-1 and -2: novel integral membranes proteins localizing at tight junctions with no sequence similarity to occludin. J. Cell Biol. **141:**1539–1550.
21. **Furuse, M., T. Hirase, M. Itoh, A. Nagafuchi, S. Yonemura, S. Tsukita, and S. Tsukita.** 1993. Occludin: a novel integral membrane protein localizing at tight junctions. J. Cell Biol. **123:**1777–1788.
22. **Gao, L., and I. G. Macara.** 2004. Isoforms of the polarity protein Par6 have distinct functions. J. Biol. Chem. **279:**41557–41562.
23. **Goldstein, B., and I. G. Macara.** 2007. The PAR proteins: fundamental players in animal cell polarization. Dev. Cell **13:**609–622.
24. **González-Mariscal, L., A. Betanzos, and A. Ávila-Flores.** 2000. MAGUK proteins: structure and role in the tight junction. Semin. Cell Dev. Biol. **11:**315–324.
25. **Guillemot, L., S. Paschoud, P. Pulimeno, A. Foglia, and S. Citi.** 2008. The cytoplasmic plaque of tight junctions: a scaffolding and signalling center. Biochim. Biophys. Acta **1778:**601–613.
26. **Gumbiner, B. M.** 1993. Breaking through the tight junction barrier. J. Cell Biol. **123:**1631–1633.
27. **Hamazaki, Y., M. Itoh, H. Sasaki, M. Furuse, and S. Tsukita.** 2002. Multi-PDZ domain protein 1 (MUPP1) is concentrated at tight junctions through its possible interaction with claudin-1 and junctional adhesion molecule. J. Biol. Chem. **277:**455–461.
28. **Henrique, D., and F. Schweisguth.** 2003. Cell polarity: the ups and downs of the Par6/aPKC complex. Curr. Opin. Gen. Dev. **13:**341–350.
29. **Hogan, B. L., A. Taylor, and E. Adamson.** 1981. Cell interactions modulate embryonal carcinoma cell differentiation into parietal or visceral endoderm. Nature **291:**235–237.
30. **Hurd, T. W., L. Gao, M. H. Roh, I. G. Macara, and B. Margolis.** 2003. Direct interaction of two polarity complexes implicated in epithelial tight junction assembly. Nat. Cell Biol. **5:**137–142.
31. **Ikenouchi, J., M. Furuse, K. Furuse, H. Sasaki, S. Tsukita, and S. Tsukita.** 2005. Tricellulin constitutes a novel barrier at tricellular contacts of epithelial cells. J. Cell Biol. **171:**939–945.
32. **Inoko, A., M. Itoh, A. Tamura, M. Matsuda, M. Furuse, and S. Tsukita.** 2003. Expression and distribution of ZO-3, a tight junction MAGUK protein, in mouse tissues. Genes Cells **8:**837–845.
33. **Itoh, M., H. Sasaki, M. Furuse, H. Ozaki, T. Kita, and S. Tsukita.** 2001. Junctional adhesion molecule (JAM) binds to PAR-3: a possible mechanism for the recruitment of PAR-3 to tight junctions. J. Cell Biol. **154:**491–497.
34. **Itoh, M., S. Yonemura, A. Nagafuchi, S. Tsukita, and S. Tsukita.** 1991. A 220-kD undercoat-constitutive protein: its specific localization at cadherin-based cell-cell adhesion sites. J. Cell Biol. **115:**1449–1462.
35. **Joberty, G., C. Petersen, L. Gao, and I. G. Macara.** 2000. The cell-polarity protein Par6 links Par3 and atypical protein kinase C to Cdc42. Nat. Cell Biol. **2:**531–539.
36. **Knust, E., and O. Bossinger.** 2002. Composition and formation of intercellular junctions in epithelial cells. Science **298:**1955–1959.
37. **Krapivinsky, G., I. Medina, L. Krapivinsky, S. Gapon, and D. E. Clapham.** 2004. SynGAP-MUPP1-CaMKII synaptic complexes regulate p38 MAP kinase activity and NMDA receptor-dependent synaptic AMPA receptor potentiation. Neuron **19:**563–574.
38. **Lanaspa, M. A., N. E. Almedia, A. Andres-Hernando, C. J. Rivard, J. M. Capasso, and T. Berl.** 2007. The tight junction protein, MUPP1, is upregulated by hypertonicity and is important in the osmotic stress response in kidney cells. Proc. Natl. Acad. Sci. USA **104:**13672–13677.
39. **Lee, S. S., B. Glaunsinger, F. Mantovani, L. Banks, and R. T. Javier.** 2000. Multi-PDZ domain protein MUPP1 is a cellular target for both adenovirus E4-ORF1 and high-risk papillomavirus type 18 E6 oncoproteins. J. Virol. **74:**9680–9693.
40. **Lemmers, C., E. Médina, M. H. Delgrossi, D. Michel, J. P. Arsanto, and A. Le Bivic.** 2002. hINADl/PATJ, a homolog of discs lost, interacts with crumbs and localizes to tight junctions in human epithelial cells. J. Biol. Chem. **277:**25408–25415.
41. **Lemmers, C., D. Michel, L. Lane-Guermonprez, M. H. Delgrossi, E. Médina, J. P. Arsanto, and A. Le Bivic.** 2004. CRB3 binds directly to Par6 and regulates the morphogenesis of tight junctions in mammalian epithelial cells. Mol. Biol. Cell **15:**1324–1333.
42. **Lin, D., A. S. Edwards, J. P. Fawcett, G. Mbamalu, J. D. Scott, and T. Pawson.** 2000. A mammalian PAR-3-PAR-6 complex implicated in Cdc42/Rac1 and aPKC signalling and cell polarity. Nat. Cell Biol. **2:**540–547.
43. **Mancini, A., A. Koch, M. Stefan, H. Niemann, and T. Tamura.** 2000. The direct association of the multiple PDZ domain containing proteins (MUPP-1) with the human c-Kit C-terminus is regulated by tyrosine kinase activity. FEBS Lett. **482:**54–58.
44. **Martìn-Padura, I., S. Lostaglio, M. Schneemann, L. Williams, M. Romano, P. Fruscella, C. Panzeri, A. Stoppacciaro, L. Ruco, A. Villa, D. Simmons, and E. Deiana.** 1998. Junctional adhesion molecule, a novel member of the immunoglobulin superfamily that distributes at intercellular junctions and modulates monocyte transmigration. J. Cell Biol. **142:**117–127.
45. **Matter, K., S. Aijaz, A. Tsapara, and M. S. Balda.** 2005. Mamalian tight junctions in the regulation of epithelial differentiation and proliferation. Curr. Opin. Cell Biol. **17:**453–458.
46. **Michel, D., J. P. Arsanto, D. Massey-Harroche, C. Béclin, J. Wijnholds, and A. Le Bivic.** 2005. PATJ connects and stabilizes apical and lateral components of tight junctions in human intestinal cells. J. Cell Sci. **118:**4049–4057.
47. **Mitic, L. L., and J. M. Anderson.** 1998. Molecular structure of tight junctions. Annu. Rev. Physiol. **60:**121–142.
48. **Miyahara, M., H. Nakanishi, K. Takahashi, K. Satoh-Horikawa, K. Tachibana, and Y. Takai.** 2000. Interaction of nectin with afadin is necessary for its clustering at cell-cell contact sites but not for its *cis* dimerization or *trans* interaction. J. Biol. Chem. **275:**613–618.
49. **Nam, S. C., and K. W. Choi.** 2003. Interaction of Par-6 and Crumbs complexes is essential for photoreceptor morphogenesis in *Drosophila*. Development **130:**4363–4372.
50. **Nam, S. C., and K. W. Choi.** 2006. Domain-specific early and late function of Dpatj in *Drosophila* photoreceptor cells. Dev. Dyn. **235:**1501–1507.
51. **Noda, Y., R. Takeya, S. Ohno, S. Naito, T. Ito, and H. Sumimoto.** 2001. Human homologues of the *Caenorhabditis elegans* cell polarity protein PAR6 as an adaptor that links the small GTPases Rac1 and Cdc42 to atypical protein kinase C. Genes Cells **6:**107–119.
52. **Perez-Moreno, M., C. Jamora, and E. Fuchs.** 2003. Orchestrating cellular signals at adherens junctions. Cell **112:**535–548.
53. **Pielage, J., T. Stork, I. Bunse, and C. Klämbt.** 2003. The *drosophila* cell survival gene *discs lost* encodes a cytoplasmic Codanin-1-like protein, not a homolog of tight junction PDZ protein Patj. Dev. Cell **5:**841–851.
54. **Ponting, C. P., C. Phillips, K. E. Davies, and D. J. Blake.** 1997. PDZ domains: targeting signalling molecules to sub-membranous sites. Bioessays **19:**469–479.
55. **Qiu, R. G., A. Abo, and G. S. Martin.** 2000. A human homolog of the *C. elegans* polarity determinant Par-6 links Rac and Cdc42 to PKCζ signaling and cell transformation. Curr. Biol. **10:**697–707.
56. **Richard, M., F. Grawe, and E. Knust.** 2006. *D*PATJ plays a role in retinal morphogenesis and protects against light-dependent degeneration of photoreceptor dells in the *Drosophila* eye. Dev. Dyn. **235:**895–907.
57. **Roh, M. H., C. Liu, S. Laurinec, and B. Margolis.** 2002. The carboxyl terminus of Zonula Occludens-3 binds and recruits a mammalian homologue of Discs Lost to tight junctions. J. Biol. Chem. **277:**17501–17509.
58. **Roh, M. H., O. Makarova, C. J. Liu, K. Shin, S. Lee, S. Laurinec, M. Goyal, R. Wiggins, and B. Margolis.** 2002. The Maguk protein, Pals1, functions as an adapter, linking mammalian homologues of Crumbs and Discs Lost. J. Cell Biol. **157:**161–172.
59. **Satoh-Horikawa, K., H. Nakanishi, K. Takahashi, M. Miyahara, M. Nishimura, K. Tachibana, A. Mizoguchi, and Y. Takai.** 2000. Nectin-3, a new member of immunoglobulin-like cell adhesion molecules that shows ho-

mophilic and heterophilic cell-cell adhesion activities. J. Biol. Chem. **275:** 10291–10299.
60. **Schneeberger, E. E., and R. D. Lynch.** 1992. Structure, function, and regulation of cellular tight junctions. Am. J. Physiol. **262:**L647–L661.
61. **Shin, K., S. Straight, and B. Margolis.** 2005. PATJ regulates tight junction formation and polarity in mammalian epithelial cells. J. Cell Biol. **168:**705–711.
62. **Shin, K., Q. Wang, and B. Margolis.** 2007. PATJ regulates directional migration of mammalian epithelial cells. EMBO Rep. **8:**158–164.
63. **Simpson, E. H., R. Suffolk, and I. J. Jackson.** 1999. Identification, sequence, and mapping of the mouse multiple PDZ domain protein gene, *Mpdz*. Genomics **59:**102–104.
64. **Sotillos, S., M. T. Díaz-Meco, E. Caminero, J. Moscat, and S. Campuzano.** 2004. DaPKC-dependent phosphorylation of Crumbs is required for epithelial cell polarity in *Drosophila*. J. Cell Biol. **166:**549–557.
65. **Staehelin, L. A.** 1974. Structure and function of intercellular junctions. Int. Rev. Cytol. **39:**191–283.
66. **Straight, S. W., K. Shin, V. C. Fogg, S. Fan, C. J. Liu, M. Roh, and B. Margolis.** 2004. Loss of PALS1 expression leads to tight junction and polarity defects. Mol. Biol. Cell **15:**1981–1990.
67. **Sugihara-Mizuno, Y., M. Adachi, Y. Kobayashi, Y. Hamazaki, M. Nishimura, T. Imai, M. Furuse, and S. Tsukita.** 2007. Molecular characterization of angiomotin/JEAP family proteins: interaction with MUPP1/Patj and their endogenous properties. Genes Cells **12:**473–486.
68. **Suzuki, A., C. Ishiyama, K. Hashiba, M. Shimizu, K. Ebnet, and S. Ohno.** 2002. aPKC kinase activity is required for the asymmetric differentiation of the premature junctional complex during epithelial cell polarization. J. Cell Sci. **115:**3565–3573.
69. **Suzuki, A., and S. Ohno.** 2006. The PAR-aPKC system: lessons in polarity. J. Cell Sci. **119:**979–987.
70. **Suzuki, A., T. Yamanaka, T. Hirose, N. Manabe, K. Mizuno, M. Shimizu, K. Akimoto, Y. Izumi, T. Ohnishi, and S. Ohno.** 2001. Atypical protein kinase C is involved in the evolutionarily conserved PAR protein complex and plays a critical role in establishing epithelia-specific structures. J. Cell Biol. **152:** 1183–1196.
71. **Takahashi, K., H. Nakanishi, M. Miyahara, K. Mandai, K. Satoh, A. Satoh, H. Nishioka, J. Aoki, A. Nomoto, A. Mizoguchi, and Y. Takai.** 1999. Nectin/PRR: an immunoglobulin-like cell adhesion molecule recruited to cadherin-based adherens junctions through interaction with afadin, a PDZ domain-containing protein. J. Cell Biol. **145:**539–549.
72. **Takai, Y., W. Ikeda, H. Ogita, and Y. Rikitake.** 2008. The immunoglobulin-like cell adhesion molecule nectin and its associated protein afadin. Annu. Rev. Cell Dev. Biol. **24:**309–342.
73. **Tanentzapf, G., and U. Tepass.** 2003. Interactions between the *crumbs*, lethal giant larvae and *bazooka* pathways in epithelial polarization. Nat. Cell Biol. **5:**46–52.
74. **Tsukita, S., M. Furuse, and M. Itoh.** 2001. Multifunctional strands in tight junctions. Nat. Rev. Mol. Cell Biol. **2:**285–293.
75. **Ullmer, C., K. Schmuck, A. Figge, and H. Lübbert.** 1998. Cloning and characterization of MUPP1, a novel PDZ domain protein. FEBS Lett. **424:** 63–68.
76. **Umeda, K., J. Ikenouchi, K. Furuse, H. Sasaki, M. Nakayama, T. Matsui, S. Tsukita, M. Furuse, and S. Tsukita.** 2006. ZO-1 and ZO-2 independently determine where claudins are polymerized into tight junction strand formation. Cell **126:**741–754.
77. **van de Pavert, S. A., A. Kantardzhieva, A. Malysheva, J. Meuleman, I. Versteeg, C. Levelt, J. Klooster, S. Geiger, M. W. Seeliger, P. Rashbass, A. Le Bivic, and J. Wijnholds.** 2004. Crumbs homologue 1 is required for maintenance of photoreceptor cell polarization and adhesion during light exposure. J. Cell Sci. **117:**4169–4177.
78. **Wang, Q., and B. Margolis.** 2007. Apical junctional complexes and cell polarity. Kidney Int. **72:**1448–1458.
79. **Wang, Q., T. W. Hurd, and B. Margolis.** 2004. Tight junction protein Par6 interacts with an evolutionarily conserved region in the amino terminus of PALS1/Stardust. J. Biol. Chem. **279:**30715–30721.
80. **Yamanaka, T., Y. Horikoshi, A. Suzuki, Y. Sugiyama, K. Kitamura, R. Maniwa, Y. Nagai, A. Yamashita, T. Hirose, H. Ishikawa, and S. Ohno.** 2001. PAR-6 regulates aPKC activity in a novel way and mediates cell-cell contact-induced formation of the epithelial junctional complex. Genes Cells **6:**721–731.